Errors due to the common ray approximations of the coupling ray theory

Luděk Klimeš & Petr Bulant

Department of Geophysics, Charles University, Ke Karlovu 3, 121 16 Praha 2, Czech Republic, Fax: +420-2-2191 1214,

E-mails: klimes@seis.karlov.mff.cuni.cz, bulant@seis.karlov.mff.cuni.cz

Summary

The equations for estimating the travel–time errors due to the isotropic and anisotropic common ray approximations of the coupling ray theory for S waves are derived and numerically tested.

Keywords

Coupling ray theory, common ray approximation, travel time, perturbation methods, seismic anisotropy, inhomogeneous media.

1. Introduction

The *coupling ray theory*, applicable at all degrees of anisotropy, from isotropic models to considerably anisotropic ones, has been proposed by Coates & Chapman (1990). The numerical algorithm for calculating the frequency–dependent complex–valued S–wave polarization vectors of the coupling ray theory has been designed by Bulant & Klimeš (2002a).

There are many commonly used *quasi–isotropic approximations* of the coupling ray theory (Pšenčík 1998a), which deteriorate the accuracy of the coupling ray theory both with increasing frequency and increasing degree of anisotropy. Most of these quasi–isotropic approximations can be avoided with minimal effort (Bulant & Klimeš 2002a; 2002b), except for the *common ray approximation* for S waves. In the common ray approximation, only one reference ray is traced for both S–wave polarizations, and both S–wave travel times are approximated by the perturbation from the common reference ray. The common ray approximation thus considerably simplifies the coding of the coupling ray theory and numerical calculations, but may introduce errors in travel times due to the perturbation. These travel–time errors can deteriorate the coupling ray theory solution at high frequencies. It is thus of principal importance for numerical applications to estimate the error due to the common ray approximation.

In the common ray approximation, the S–wave travel times are usually approximated by the linear perturbation from the common reference ray. The errors of S–wave travel times may then be approximated by second–order perturbations. The calculation of these estimates of travel–time errors due to the *isotropic common ray approximation* and the *anisotropic common ray approximation* (Bakker 2002) is proposed and numerically demonstrated in this paper. The equations for estimating the travel–time errors due to the isotropic and anisotropic common ray approximations of the coupling ray theory for S waves are derived in a form suitable for dynamic ray tracing in ray–centred (Riemannian normal) coordinates.

In: Seismic Waves in Complex 3-D Structures, Report 12 (Department of Geophysics, Charles University, Prague, 2002), pp. 185–212

2. Common ray approximations

For the derivation of the coupling ray theory refer to Coates & Chapman (1990) and Červený (2001). For the description of the numerical algorithm refer to Červený (2001) and Bulant & Klimeš (2002a). Here we shall concentrate only on estimating the travel–time errors due to the common ray approximations. The estimates are based on the equations for the second–order perturbations of travel time derived by Klimeš (2002).

2.1. Selection of the reference ray

The isotropic ray theory is always the limiting case of the coupling ray theory for decreasing anisotropy at a fixed frequency. On the other hand, the high–frequency limit of the coupling ray theory at a fixed anisotropy depends on the choice of the reference ray, and even on the choice of the *system* of reference rays, because the amplitudes are determined by the paraxial reference rays.

The reference ray should be close to the ray of the wave under study. In particular, the reference ray is best represented by the *anisotropic ray theory reference ray*, with the initial condition for the vectorial amplitude given by the relevant eigenvector of the Christoffel matrix corresponding to the reference ray. Then the travel time of the selected polarization is exact, and only the travel–time difference between the S–wave polarizations is approximate. The coupling ray theory may then also be used at high frequencies because the approximate travel–time difference influences only the coupling due to low–frequency scattering. The coupling ray theory then correctly limits to the anisotropic ray theory for high frequencies. For other choices of reference rays, the high–frequency limit of the coupling ray theory at a fixed anisotropy is incorrect, although the differences may be small at the finite frequencies under consideration.

In the *anisotropic common ray approximation*, the common reference ray is traced using the averaged Hamiltonian of both S–wave polarizations (Bakker 2002).

In the less accurate *isotropic common ray approximation*, the reference ray is traced in the reference isotropic model. Moreover, the reference isotropic model may be selected in different ways, yielding quasi–isotropic approximations of various accuracy.

2.2. Linear perturbation of travel time

Let $a_{ijkl} = a_{ijkl}(x_m)$ be the density–normalized elastic moduli describing a *smooth anisotropic model*, and $v_0 = v_0(x_m)$ the velocity in the smooth *reference isotropic model* used to trace the reference rays. We shall abbreviate v_0 as the reference velocity.

Assume a phase–space *reference ray*, parametrized by reference travel time τ, with reference slowness vectors $p_i(\tau)$ known at all its points $x_j(\tau)$. Using the reference slowness vectors, we can calculate reference Christoffel matrix

$$\Gamma_{jk}(\tau) = p_i(\tau)\, a_{ijkl}(x_m(\tau))\, p_l(\tau) \tag{1}$$

and its eigenvectors $g_{i\alpha}(\tau)$, $\alpha = 1,2,3$ along the reference ray. Whereas the Einstein summation over the pairs of identical Roman indices (both subscripts and superscripts) $i,j,k,... = 1,2,3$ or $I,J,K,... = 1,2$ is used throughout this paper, no implicit summation applies to Greek subscripts $\alpha,\beta,...$ indexing the eigenvectors of the Christoffel matrix. Assume that eigenvectors $g_{i1}(\tau)$ and $g_{i2}(\tau)$ correspond to the S waves, and eigenvector $g_{i3}(\tau)$ to the P wave. The eigenvectors should vary continuously along the reference ray (Vavryčuk 2001, Bulant & Klimeš 2002a).

Let us denote $\tau_\alpha(\tau)$ the travel time corresponding to the selected polarization $g_{i\alpha}(\tau)$. It may be approximated by a quadrature along the unperturbed reference ray,

$$\frac{\mathrm{d}\tau_\alpha}{\mathrm{d}\tau} = [\Gamma_{jk} g_{j\alpha} g_{k\alpha}]^{-\frac{1}{2}} \quad . \tag{2}$$

Travel–time approximation (2), suggested for the coupling ray theory by Bulant & Klimeš (2002a), would become exact for a reference ray following the path of the exact ray. Travel–time approximation (2) can be derived as the linear perturbation corresponding to Hamiltonian

$$H_\alpha(x_m, p_n) = -[G_\alpha(x_m, p_n)]^{-\frac{1}{2}} \quad , \tag{3}$$

where $G_\alpha(x_m, p_n)$ is the eigenvalue of Christoffel matrix (1), corresponding to polarization $g_{i\alpha}$ (Klimeš 2002, eqs. 43 and 65).

2.3. Reference isotropic Hamiltonian and correct anisotropic Hamiltonians

Hamiltonian (3), specified for the reference isotropic medium, reads

$$H_0(x_m, p_n) = -[v_0(x_m)]^{-1}(p_i p_i)^{-\frac{1}{2}} \quad . \tag{4}$$

The value of Hamiltonian (4) at the reference ray is

$$H_0 = -1 \quad . \tag{5}$$

Partial derivatives with respect to the coordinates, denoted by Roman subscripts following a comma, of Hamiltonian (4) are

$$H_{0,i} = v_{0,i}(v_0)^{-2}(p_i p_i)^{-\frac{1}{2}} \quad , \tag{6}$$

which is, at the reference ray, equal to

$$\boxed{H_{0,i} = v_{0,i}(v_0)^{-1} \quad . \qquad (7)}$$

Partial derivatives with respect to the components of the slowness vector, denoted by Roman superscripts following a comma, of Hamiltonian (4) are

$$H_0^{,i} = (v_0)^{-1}(p_k p_k)^{-\frac{3}{2}} p_i \quad , \tag{8}$$

which is, at the reference ray, equal to

$$H_0^{,i} = (v_0)^2 p_i \quad . \tag{9}$$

The second–order partial derivatives of Hamiltonian (4) with respect to the components of the slowness vector are

$$H_0^{,ij} = (v_0)^{-1}(p_k p_k)^{-\frac{3}{2}}\,\delta^{ij} - 3\,(v_0)^{-1}(p_k p_k)^{-\frac{5}{2}}\,p_i p_j \quad , \tag{10}$$

which is, at the reference ray, equal to

$$H_0^{,ij} = (v_0)^2\,\delta^{ij} - 3\,(v_0)^4\,p_i p_j \quad . \tag{11}$$

Kronecker symbol δ^{ij} denotes the components of the identity matrix.

The value of Hamiltonian (3), corresponding to unit eigenvector $g_{i\alpha}$ of the Christoffel matrix, at the reference ray, is

$$\boxed{H_\alpha = -(a_{ijkl} g_{i\alpha} p_j g_{k\alpha} p_l)^{-\frac{1}{2}} \quad . \qquad (12)}$$

Partial derivatives of Hamiltonian (4) with respect to the coordinates are

$$\boxed{H_{\alpha,i} = -\tfrac{1}{2}(H_\alpha)^3 a_{mjkl,i} g_{m\alpha} p_j g_{k\alpha} p_l \quad . \qquad (13)}$$

Partial derivatives of Hamiltonian (4) with respect to the components of the slowness vector are

$$\boxed{H_\alpha^{;i} = -(H_\alpha)^3 a_{mikl} g_{m\alpha} g_{k\alpha} p_l \quad . \qquad (14)}$$

The values of phase–space derivatives (13) and (14) are evaluated at the reference ray in this paper. Partial derivatives (14) satisfy Euler's relation

$$H_\alpha^{;i} p_i = -H_\alpha \tag{15}$$

for a homogeneous function of the minus first degree.

The quantities enclosed above in boxes are necessary for estimating the errors due to the common ray approximations of the coupling ray theory.

2.4. Parametric system of the Hamiltonians and errors due to the common ray approximations

We consider the two–parametric set $H = H(x_m, p_n, f_\alpha)$ of Hamiltonians parametrized by f_α, $\alpha = 1, 2$ for an S wave, or the one–parametric set $H = H(x_m, p_n, f_\alpha)$ of Hamiltonians parametrized by f_α, $\alpha = 3$ for a P wave,

$$H(x_m, p_n, f_\alpha) = H_0(x_m, p_n) + \sum_\alpha [H_\alpha(x_m, p_n) - H_0(x_m, p_n)]\; f_\alpha \quad . \tag{16}$$

Parametric system (16) of the Hamiltonians then generates parametric system $\tau(x_m, f_\alpha)$ of travel time fields corresponding to the individual Hamiltonians $H(x_m, p_n, f_\alpha)$.

For an S wave, we obtain the Hamiltonian corresponding to the isotropic common ray approximation in the reference isotropic model for $(f_1, f_2) = (0, 0)$, the Hamiltonian corresponding to the first anisotropic S–wave polarization for $(f_1, f_2) = (1, 0)$, the Hamiltonian corresponding to the second anisotropic S–wave polarization for $(f_1, f_2) = (0, 1)$, and the averaged Hamiltonian of both S–wave polarizations corresponding to the anisotropic common ray approximation by Bakker (2002) for $(f_1, f_2) = (\frac{1}{2}, \frac{1}{2})$.

For a P wave, we obtain the Hamiltonian corresponding to the reference ray in the reference isotropic model for $f_3 = 0$, and the Hamiltonian corresponding to the anisotropic P wave for $f_3 = 1$.

The second–order Taylor expansion of travel time with respect to parameters f_α is

$$\tau(\bullet, f_\alpha) \approx \tau + \sum_\alpha \tau_{,\alpha} f_\alpha + \tfrac{1}{2} \sum_\alpha \sum_\beta \tau_{,\alpha\beta} f_\alpha f_\beta \quad , \tag{17}$$

where the Greek subscripts following a comma denote the derivatives with respect to parameters f_α, also called *perturbations*. Here travel time τ and its perturbations $\tau_{,\alpha}$, $\tau_{,\alpha\beta}$ written without arguments f_α correspond to the reference model $f_\alpha = 0$. Travel–time approximation (2) corresponds to the linear part of Taylor expansion (17). The error of travel–time approximation (2) may thus be approximated by the second–order term in Taylor expansion (17).

We may now express the estimates of the travel–time errors due to the *isotropic common ray* (ICR) *approximation* of anisotropic travel times in terms of the second–order perturbations of travel time. The errors of travel–time approximation (2) from isotropic common reference ray $(f_1, f_2) = (0, 0)$ to the correct anisotropic S–wave ray $(f_1, f_2) = (1, 0)$ and to the correct anisotropic S–wave ray $(f_1, f_2) = (0, 1)$ are approximately

$$\boxed{\delta\tau_\alpha^{\mathrm{ICR}} = \frac{\tau_{,\alpha\alpha}}{2} \quad , \qquad (18)}$$

where $\alpha = 1, 2$ for S waves. Equation (18) with $\alpha = 3$ gives analogously the estimate of the error of travel–time approximation (2) from isotropic reference P–wave ray $f_3 = 0$ to the correct anisotropic P–wave ray $f_3 = 1$.

We may also use the second–order perturbations of travel time, calculated along the isotropic common reference ray, to estimate the accuracy of the *anisotropic common ray* (ACR) *approximation* (Bakker 2002). The estimates of errors of travel–time approximation (2) from anisotropic S–wave common reference ray $(f_1, f_2) = (\frac{1}{2}, \frac{1}{2})$ to $(f_1, f_2) = (1, 0)$ and to $(f_1, f_2) = (0, 1)$ are equal,

$$\boxed{\delta\tau_\alpha^{\mathrm{ACR}} = \frac{\tau_{,11} - 2\tau_{,12} + \tau_{,22}}{8} \quad , \qquad (19)}$$

where $\alpha = 1, 2$. Error estimates (19) represent the contributions of the quadratic terms in Taylor expansion (17) at the distances from the anisotropic S–wave common reference ray to the correct S–wave rays.

To calculate the first–order and second–order perturbations $\tau_{,\alpha}$ and $\tau_{,\alpha\beta}$ of travel time, we shall need the the first–order and second–order phase–space derivatives and perturbations of the Hamiltonian. The phase–space derivatives and perturbations of Hamiltonian (16) in the reference model $f_\alpha = 0$ are

$$H_{,i} = H_{0,i} \quad , \qquad (20)$$

$$H^{,i} = H_0^{,i} \quad , \qquad (21)$$

$$H^{,ij} = H_0^{,ij} \quad , \qquad (22)$$

$$H_{,\alpha} = H_\alpha - H_0 \quad , \qquad (23)$$

$$H_{,i\alpha} = H_{\alpha,i} - H_{0,i} \quad , \qquad (24)$$

$$H_{,\alpha}^{,i} = H_\alpha^{,i} - H_0^{,i} \quad , \qquad (25)$$

$$H_{,\alpha\beta} = 0 \quad , \qquad (26)$$

where the Greek subscripts following a comma denote the derivatives with respect to parameters f_α, analogously as for travel time.

2.5. Dynamic ray tracing and ray–centred coordinates

We define the matrices of the partial derivatives of coordinates x_i and of the slowness–vector components $p_i = \tau_{,i}$ with respect to 3 *ray parameters*: ray take–off parameters γ_1, γ_2, and independent parameter $\gamma_3 = \tau$ along rays,

$$Q_{ia} = \frac{\partial x_i}{\partial \gamma_a} \quad , \qquad P_{ia} = \frac{\partial \tau_{,i}}{\partial \gamma_a} \quad . \tag{27}$$

Matrices Q_{ia} and P_{ia} can be calculated by solving numerically a set of linear ordinary differential equations called the *dynamic ray tracing equations* (Babich & Buldyrev 1972; Červený 1972; Arnaud 1973; Červený & Hron 1980). Matrices Q_{ia} and P_{ia} describe, by definition, the properties of the orthonomic system of rays corresponding to the travel time under consideration. They may be expressed in terms of their initial values and the paraxial ray propagator matrix (Červený 2001).

The second–order spatial derivatives $\tau_{,ij}$ of travel time can be expressed in terms of the transformation matrices Q_{ia} and P_{ia} from ray parameters γ_a to phase–space coordinates x_i, p_i. Equation

$$P_{ia} = \tau_{,ij}\ Q_{ja} \tag{28}$$

is a direct consequence of above definitions (27).

Let us denote by h_{i1}, h_{i2}, h_{i3} the basis vectors of the *ray–centred coordinate system* (Riemannian normal coordinate system) proposed by Luneburg (1944), Babich & Buldyrev (1972) and Popov & Pšenčík (1978a; 1978b). The orthonormal basis vectors of the ray–centred coordinate system are calculated along the reference ray in the reference isotropic model. The first two basis vectors h_{iM} of the ray–centred coordinate system are tangent to the wavefront, the third basis vector $h_{i3} = v_0 p_i$ is tangent to the ray. The equations for calculating the basis vectors of the ray–centred coordinate system can be found, e.g., in the book by Červený (2001).

The quantities covariantly transformed from spatial coordinates x_i to the local Cartesian basis h_{im} of the ray–centred coordinate system are marked by a tilde $\widetilde{\ }$. In particular,

$$\widetilde{Q}_{ia} = h_{mi} Q_{ma} \quad , \tag{29}$$

$$\widetilde{P}_{ia} = h_{mi} P_{ma} \quad , \tag{30}$$

$$\widetilde{\tau}_{,ij} = h_{mi} \tau_{,mn} h_{nj} \quad , \tag{31}$$

$$\widetilde{\tau}_{,i\alpha} = h_{mi} \tau_{,m\alpha} \quad , \tag{32}$$

$$\boxed{\begin{aligned} \widetilde{H}_{0,i} &= H_{0,m} h_{mi} \quad , & (33)\\ \widetilde{H}_{\alpha,i} &= H_{\alpha,m} h_{mi} \quad , & (34)\\ \widetilde{H}_{\alpha}^{;i} &= H_{\alpha}^{;m} h_{mi} \quad . & (35) \end{aligned}}$$

Since we consider matrices Q_{ia} and P_{ia} defined for $\gamma_3 = \tau$,

$$\widetilde{Q}_{3J} = 0 \quad . \tag{36}$$

The 2×2 submatrices $\widetilde{Q}_{IJ}$ and $\widetilde{P}_{IJ}$ of matrices (29) and (30) are usually calculated by the *dynamic ray tracing equations in ray–centred coordinates* (Červený 2001, eq. 4.1.65),

$$\frac{\mathrm{d}}{\mathrm{d}\tau} \widetilde{Q}_{IJ} = (v_0)^2\ \widetilde{P}_{IJ} \quad . \tag{37}$$

$$\frac{\mathrm{d}}{\mathrm{d}\tau}\widetilde{P}_{IJ} = -(v_0)^{-1}\widetilde{(v_0)}_{,IK}\widetilde{Q}_{KJ} \quad , \tag{38}$$

where

$$\widetilde{(v_0)}_{,IK} = h_{mI}\,(v_0)_{,mn}\,h_{nJ} \tag{39}$$

are the second–order velocity derivatives in ray–centred coordinates.

We shall thus express the equations for estimating the travel–time errors due to the common ray approximations of the coupling ray theory in terms of the 2×2 matrices $\widetilde{Q}_{IJ}$ and $\widetilde{P}_{IJ}$ in ray–centred coordinates.

2.6. First–order perturbations of the travel–time gradient

To calculate the second–order perturbations of travel time, we need to know at least the ray–normal projection

$$\tau^{\perp}_{,i\alpha} = E^{\perp}_{ij}\tau_{,j\alpha} \tag{40}$$

of the first–order perturbations $\tau_{,i\alpha}$ of the travel–time gradient. The ray–normal projection matrix $E^{\perp}_{ij}$ can be expressed in terms of the first two basis vectors of the ray–centred coordinate system,

$$E^{\perp}_{ij} = h_{iM}h_{jM} \quad . \tag{41}$$

The covariant transform (Klimeš 2002, eq. 69)

$$T^{\perp}_{J\alpha} = \tau^{\perp}_{,i\alpha}\,Q_{iJ} \tag{42}$$

of ray–normal derivatives (40) into ray parameters can be determined by numerical quadrature (Klimeš 2002, eq. 75)

$$\boxed{T^{\perp}_{J\alpha}(\tau) = T^{\perp}_{J\alpha}(\tau^0) + \int_{\tau^0}^{\tau}\mathrm{d}\tau\, K^{\perp}_{i\alpha}Q_{iJ}} \tag{43}$$

along the reference ray, with zero initial conditions $T^{\perp}_{J\alpha}(\tau^0) = 0$ at the point source.

The ray–normal integration kernel for the perturbations of the travel–time gradient is (Klimeš 2002, eq. 80)

$$K^{\perp}_{i\alpha} = E^{\perp}_{ia}\,(-H_{,a\alpha} + H_{,a}\,H^{;r}_{,\alpha}\,p_r) - H^{;r}_{,\alpha}\,\tau^{\perp}_{,ri} \quad , \tag{44}$$

where

$$\tau^{\perp}_{,ij} = E^{\perp}_{ia}E^{\perp}_{jb}\tau_{,ab} \tag{45}$$

is the ray–normal projection of the second–order derivatives $\tau_{,ij}$ of travel time.

Inserting equations (20), (24), (25) with (9) and (15), and (45) into (44), we arrive at

$$K^{\perp}_{i\alpha} = -E^{\perp}_{ia}\,(H_{\alpha,a} + H_{\alpha}H_{0,a}) - H^{;r}_{\alpha}\,E^{\perp}_{ra}\tau_{,ab}E^{\perp}_{bi} \quad . \tag{46}$$

Multiplying equation (46) by the first two columns Q_{iJ} of the matrix of geometrical spreading, inserting equation (41), and considering transforms (29), (30), (31) and relations (28) and (36), we arrive at

$$\boxed{K^{\perp}_{i\alpha}Q_{iJ} = -(\widetilde{H}_{\alpha,I} + H_{\alpha}\widetilde{H}_{0,I})\widetilde{Q}_{IJ} - \widetilde{H}^{;I}_{\alpha}\widetilde{P}_{IJ} \quad ,} \tag{47}$$

where $\widetilde{Q}_{IJ}$ and $\widetilde{P}_{IJ}$ are the 2×2 submatrices of matrices (29) and (30). The 2×2 matrices $\widetilde{Q}_{IJ}$ and $\widetilde{P}_{IJ}$ are usually calculated by the dynamic ray tracing equations (37) and (38) in ray–centred coordinates.

Inserting equations (40) and (41) into (42) while considering transforms (29) and (32), we arrive at

$$T^{\perp}_{J\alpha} = \widetilde{\tau}_{,I\alpha}\,\widetilde{Q}_{IJ} \quad . \tag{48}$$

Then the first–order perturbations of the travel–time gradient expressed in ray–centred coordinates are

$$\boxed{\widetilde{\tau}_{,I\alpha} = T^{\perp}_{J\alpha}\widetilde{Q}^{-1}_{JI} \quad ,} \tag{49}$$

where $\widetilde{Q}^{-1}_{JI}$ are the components of the matrix inverse to 2×2 matrix $\widetilde{Q}_{IJ}$ calculated by dynamic ray tracing (37) and (38) in ray–centred coordinates.

The value of $\widetilde{\tau}_{,I\alpha}$ at the point source, where $T^{\perp}_{J\alpha}(\tau^0)=0$ and $\widetilde{Q}_{IJ}(\tau^0)=0$, can be obtained by the l'Hospital rule with respect to $\tau\to\tau^0+$,

$$\widetilde{\tau}_{,I\alpha}(\tau^0) = -(v_0)^{-2}\widetilde{H}^{;I}_{\alpha} \quad . \tag{50}$$

2.7. Second–order perturbations of travel time

The second–order perturbations of travel time can be determined by numerical quadrature (Klimeš 2002, eqs. 19 and 20)

$$\boxed{\tau_{,\alpha\beta}(\tau) = \tau_{,\alpha\beta}(\tau^0) + \int_{\tau^0}^{\tau}\mathrm{d}\tau\; K_{\alpha\beta}} \tag{51}$$

along the reference ray, with zero initial conditions $\tau_{,\alpha\beta}(\tau^0)=0$ at the point source.

For Hamiltonian (3), the integration kernel for the second–order perturbations of travel time can be expressed as (Klimeš 2002, eq. 64)

$$K_{\alpha\beta} = -H_{,\alpha\beta} - H^{;i}_{,\alpha}\tau^{\perp}_{,i\beta} - H^{;i}_{,\beta}\tau^{\perp}_{,i\alpha} - H^{,ij}\tau^{\perp}_{,i\alpha}\tau^{\perp}_{,j\beta} \quad . \tag{52}$$

Inserting relations (22) with (11), (25) with (9), and (26), equation (52) becomes

$$K_{\alpha\beta} = -H^{;i}_{\alpha}\tau^{\perp}_{,i\beta} - H^{;i}_{\beta}\tau^{\perp}_{,i\alpha} - (v_0)^2\tau^{\perp}_{,i\alpha}\tau^{\perp}_{,i\beta} \quad . \tag{53}$$

Inserting relations (40) and (41), and considering transforms (32) and (35), equation (53) can be expressed in ray–centred coordinates as

$$\boxed{K_{\alpha\beta} = -\widetilde{H}^{;I}_{\alpha}\widetilde{\tau}_{,I\beta} - \widetilde{H}^{;I}_{\beta}\widetilde{\tau}_{,I\alpha} - (v_0)^2\widetilde{\tau}_{,I\alpha}\widetilde{\tau}_{,I\beta} \quad .} \tag{54}$$

Equation (51) cannot be integrated numerically in the vicinities of caustics where $\widetilde{Q}_{IJ}$ is singular and $\widetilde{\tau}_{,I\alpha}$ in integration kernel (54) thus approach infinity. Fortunately, we may convert equation (51) analogously to Klimeš (2002, sec. 4.2), but in ray–centred coordinates. Equation (51) with integration kernel (54) may be converted using dynamic ray tracing equations (37) and (38) and equation (43) with (47) into

$$\boxed{\tau_{,\alpha\beta}(\tau) = \tau_{,\alpha\beta}(\tau^0) + \left[T^{\perp}_{I\alpha}\widetilde{Q}^{-1}_{IK}\widetilde{P}^{-1}_{JK}T^{\perp}_{J\beta}\right]^{\tau}_{\tau^0} + \int_{\tau^0}^{\tau}\mathrm{d}\tau\; K^{\mathrm{caust}}_{\alpha\beta}} \tag{55}$$

with modified integration kernel

$$\boxed{\begin{aligned} K^{\mathrm{caust}}_{\alpha\beta} =& (\widetilde{H}_{\alpha,I} + H_{\alpha}\widetilde{H}_{0,I})\,T^{\perp}_{J\beta}\widetilde{P}^{-1}_{JI} \\ &+ (\widetilde{H}_{\beta,I} + H_{\beta}\widetilde{H}_{0,I})\,T^{\perp}_{J\alpha}\widetilde{P}^{-1}_{JI} - (v_0)^{-1}\widetilde{(v_0)}_{,KL}T^{\perp}_{I\alpha}\widetilde{P}^{-1}_{IK}T^{\perp}_{J\beta}\widetilde{P}^{-1}_{JL} \quad . \end{aligned}} \tag{56}$$

Combining equations (51) and (55) enables the optimization of calculating the second–order perturbations of travel time by numerical quadrature.

The second–order perturbations of travel time calculated by quadratures (51) and (55) can be inserted into equation (18) for the travel–time errors due to the isotropic common ray approximation, and into equation (19) for the travel–time errors due to the anisotropic common ray approximation.

3. Numerical example

The calculation of the first–order P–wave travel–time perturbations from a reference isotropic model to an anisotropic model and the calculation of the S–wave coupling ray theory travel–time and amplitude corrections along the isotropic reference rays have been coded and added to the Fortran 77 package CRT (Bucha & Bulant 2002).

The new version 5.60 of package CRT have been supplemented by the calculation of the second–order perturbations of travel times, which enables (a) the errors due to the isotropic common ray approximation of the coupling ray theory to be estimated, (b) the errors due to the anisotropic common ray approximation of the coupling ray theory to be estimated (c) the results of the coupling ray theory with the anisotropic reference rays to be approximately simulated for testing purposes.

3.1. Model QI

A vertically heterogeneous 1-D anisotropic model QI (model WA rotated by 45°) was provided by Pšenčík & Dellinger (2001) who performed the coupling ray theory calculations using the programs of package ANRAY (Pšenčík 1998b) and compared the results with the anisotropic reflectivity calculations. The density–normalized elastic moduli a_{ijkl} at the surface (zero depth) are

$$\begin{array}{c} \\ 11 \\ 22 \\ 33 \\ 23 \\ 13 \\ 12 \end{array} \begin{array}{c} \begin{array}{cccccc} 11 & 22 & 33 & 23 & 13 & 12 \end{array} \\ \left(\begin{array}{cccccc} 14.48500 & 4.52500 & 4.75000 & 0.00000 & 0.00000 & -0.58000 \\ & 14.48500 & 4.75000 & 0.00000 & 0.00000 & -0.58000 \\ & & 15.71000 & 0.00000 & 0.00000 & -0.29000 \\ & & & 5.15500 & -0.17500 & 0.00000 \\ & & & & 5.15500 & 0.00000 \\ & & & & & 5.04500 \end{array}\right) \end{array} \tag{57}$$

and at the depth of 1 length unit they are

$$\begin{array}{c} \\ 11 \\ 22 \\ 33 \\ 23 \\ 13 \\ 12 \end{array} \begin{array}{c} \begin{array}{cccccc} 11 & 22 & 33 & 23 & 13 & 12 \end{array} \\ \left(\begin{array}{cccccc} 22.08963 & 6.90063 & 7.24375 & 0.00000 & 0.00000 & -0.88450 \\ & 22.08963 & 7.24375 & 0.00000 & 0.00000 & -0.88450 \\ & & 23.95775 & 0.00000 & 0.00000 & -0.44225 \\ & & & 7.86138 & -0.26688 & 0.00000 \\ & & & & 7.86138 & 0.00000 \\ & & & & & 7.69363 \end{array}\right) \end{array} . \tag{58}$$

The reference isotropic model is given by

$$v_{\mathrm{P}}^2 = 15.00 \quad , \qquad v_{\mathrm{S}}^2 = 5.10 \tag{59}$$

at the surface, and

$$v_{\mathrm{P}}^2 = 23.00 \quad , \qquad v_{\mathrm{S}}^2 = 7.79 \tag{60}$$

at the depth of 1 length unit. All the above values are interpolated linearly with depth. The homogeneous density is $\rho = 1$.

The synthetic seismograms, corresponding to vertical force $\mathbf{F} = (0,0,100)^{\mathrm{T}}$ at position $(50,50,0)^{\mathrm{T}}$, are calculated at 29 receivers $(51,50,0.010)^{\mathrm{T}}$, $(51,50,0.030)^{\mathrm{T}}$, $(51,50,0.050)^{\mathrm{T}}$, ..., $(51,50,0.570)^{\mathrm{T}}$ located in a vertical well. The source time function is the Gabor signal $\cos(2\pi ft)\exp[-(2\pi ft/4)^2]$ with reference frequency $f = 50\,\mathrm{Hz}$, band–pass filtered by a cosine filter given by frequencies 0 Hz, 5 Hz, 60 Hz and 100 Hz.

The data for model QI may be found on the compact disks of Bucha, Bulant & Klimeš (2001) and Bucha & Bulant (2002) together with the Fortran 77 source code of packages CRT (Červený, Klimeš & Pšenčík 1988) and ANRAY (Gajewski & Pšenčík 1990, Pšenčík 1998b). For comparison with the isotropic and anisotropic ray theory seismograms in model QI and for a more detailed discussion and description of this model refer to Pšenčík & Dellinger (2001).

3.2. Models QI2, QI4 and QI8

To emphasize the effects of perturbations of travel time, new models with an increased degree of anisotropy have been derived from the QI model.

The differences of the elastic moduli of model **QI2** from the elastic moduli of the reference isotropic model (59), (60) are exactly twice larger than the differences of model QI. The density–normalized elastic moduli a_{ijkl} of model QI2 at the surface (zero depth) are

$$\begin{array}{cc} & \begin{array}{cccccc} 11 & 22 & 33 & 23 & 13 & 12 \end{array} \\ \begin{array}{c} 11 \\ 22 \\ 33 \\ 23 \\ 13 \\ 12 \end{array} & \begin{pmatrix} 13.97000 & 4.25000 & 4.70000 & 0.00000 & 0.00000 & -1.16000 \\ & 13.97000 & 4.70000 & 0.00000 & 0.00000 & -1.16000 \\ & & 16.42000 & 0.00000 & 0.00000 & -0.58000 \\ & & & 5.21000 & -0.35000 & 0.00000 \\ & & & & 5.21000 & 0.00000 \\ & & & & & 4.99000 \end{pmatrix} \end{array} \tag{61}$$

and at the depth of 1 length unit they are

$$\begin{array}{cc} & \begin{array}{cccccc} 11 & 22 & 33 & 23 & 13 & 12 \end{array} \\ \begin{array}{c} 11 \\ 22 \\ 33 \\ 23 \\ 13 \\ 12 \end{array} & \begin{pmatrix} 21.17926 & 6.38126 & 7.06750 & 0.00000 & 0.00000 & -1.76900 \\ & 21.17926 & 7.06750 & 0.00000 & 0.00000 & -1.76900 \\ & & 24.91550 & 0.00000 & 0.00000 & -0.88450 \\ & & & 7.93276 & -0.53376 & 0.00000 \\ & & & & 7.93276 & 0.00000 \\ & & & & & 7.59726 \end{pmatrix} \end{array} . \tag{62}$$

Analogously, the differences of the elastic moduli of model **QI4** from the elastic moduli of the reference isotropic model (59), (60) are exactly 4 times larger than the differences of model QI. The density–normalized elastic moduli a_{ijkl} of model QI4 at the surface (zero depth) are

$$\begin{array}{cc} & \begin{array}{cccccc} 11 & 22 & 33 & 23 & 13 & 12 \end{array} \\ \begin{array}{c} 11 \\ 22 \\ 33 \\ 23 \\ 13 \\ 12 \end{array} & \begin{pmatrix} 12.94000 & 3.70000 & 4.60000 & 0.00000 & 0.00000 & -2.32000 \\ & 12.94000 & 4.60000 & 0.00000 & 0.00000 & -2.32000 \\ & & 17.84000 & 0.00000 & 0.00000 & -1.16000 \\ & & & 5.32000 & -0.70000 & 0.00000 \\ & & & & 5.32000 & 0.00000 \\ & & & & & 4.88000 \end{pmatrix} \end{array} . \tag{63}$$

and at the depth of 1 length unit they are

$$\begin{array}{c} \\ 11\\22\\33\\23\\13\\12 \end{array}\begin{array}{c} \begin{array}{cccccc} 11 & 22 & 33 & 23 & 13 & 12 \end{array} \\ \begin{pmatrix} 19.35852 & 5.34252 & 6.71500 & 0.00000 & 0.00000 & -3.53800 \\ & 19.35852 & 6.71500 & 0.00000 & 0.00000 & -3.53800 \\ & & 26.83100 & 0.00000 & 0.00000 & -1.76900 \\ & & & 8.07552 & -1.06752 & 0.00000 \\ & & & & 8.07552 & 0.00000 \\ & & & & & 7.40452 \end{pmatrix} \end{array} . \tag{64}$$

Note that the perturbation approach cannot be applied to model **QI8**, in which the differences of the elastic moduli from the elastic moduli of the reference isotropic model (59), (60) are exactly 8 times larger than the differences of model QI. Taylor expansion (17) with respect to the perturbations of the Hamiltonian does not seem to converge reasonably in model QI8.

3.3. Effects of quasi–isotropic approximations of reference rays

The coupling ray theory synthetic seismograms in model QI corresponding to the anisotropic ray theory reference rays have been approximated by the second–order perturbation of travel time along isotropic rays. They are compared with the seismograms calculated by the isotropic common ray approximation of the coupling ray theory in Figure 1. The alteration of the seismograms due to the isotropic common ray approximation is scarcely observable in model QI. To make the alteration of the seismograms due to the isotropic common ray approximation more visible, an analogous comparison, but in model QI2, is shown in Figure 2. The first–order isotropic common ray approximation is considerably inaccurate in model QI4, see the seismograms of Figure 3.

The individual terms in the second–order Taylor expansion (17) of the anisotropic ray theory travel times in the vicinity of isotropic common rays are displayed in Tables 1, 2 and 3, for models QI, QI2 and QI4, respectively. The differences between the second–order Taylor expansion (17) and the anisotropic ray theory travel times calculated by program ANRAY version 4.40 are also given. The quadratic terms (18) in Taylor expansion (17) represent the estimates of the errors due to the isotropic common ray (ICR) approximation of the anisotropic ray theory travel times. Also shown is estimate (19) of the errors due to the anisotropic common ray (ACR) approximation. Only the results at the 1^{st}, 8^{th}, 15^{th}, 22^{nd} and 29^{th} receivers are shown, because the variation of the quantities along the vertical profile in models QI, QI2 and QI4 is very moderate.

The maximum travel–time error of 0.000258 seconds of the isotropic common ray approximation in model QI corresponds to the wavefield relative error of 8.1% at 50 Hz.

The maximum travel–time error of 0.001001 seconds of the isotropic common ray approximation in model QI2 is clearly visible on the left–hand side of Figure 2, and corresponds to the wavefield relative error of 31% at 50 Hz. The accuracy of the anisotropic common ray approximation by Bakker (2002) in model QI2 would be even better than the accuracy of the isotropic common ray approximation in model QI, see Tables 1 and 2.

The first–order isotropic common ray approximation is considerably inaccurate in model QI4, see Figure 3 and Table 3. The inaccuracy of the second–order Taylor expansion (17) of travel time in model QI4 roughly corresponds to the line thickness

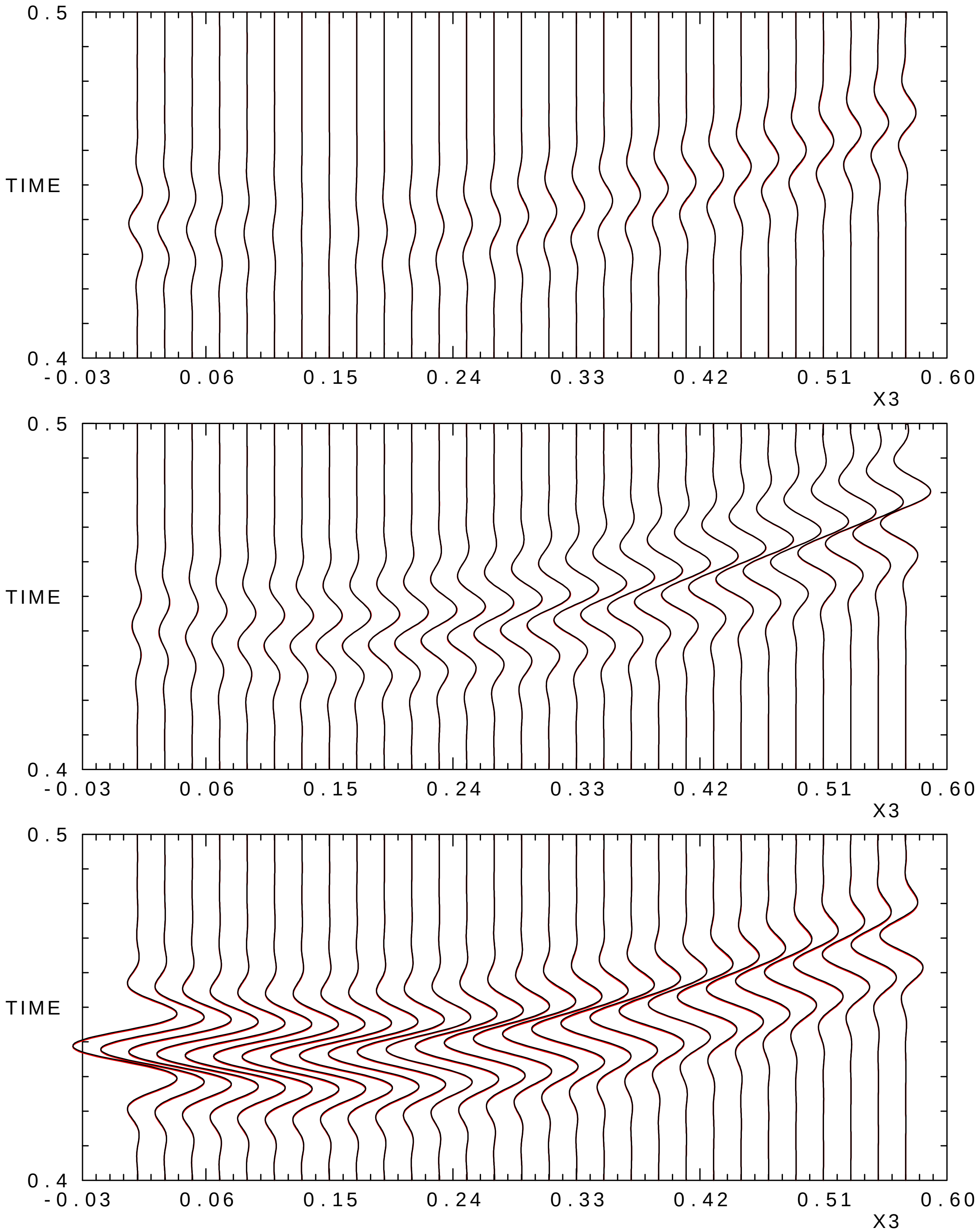

Figure 1. Coupling ray theory synthetic seismograms in model QI. The **black** seismograms correspond to the *anisotropic reference rays*, simulated by the second–order perturbation of travel time along isotropic rays. The **red** seismograms correspond to the *isotropic common ray* approximation of the coupling ray theory, and are mostly obscured by the black seismograms. From top to bottom: the first (radial) component, the second (transverse) component, the third (vertical) component. Note that the second component is zero in the one–dimensional reference isotropic model.

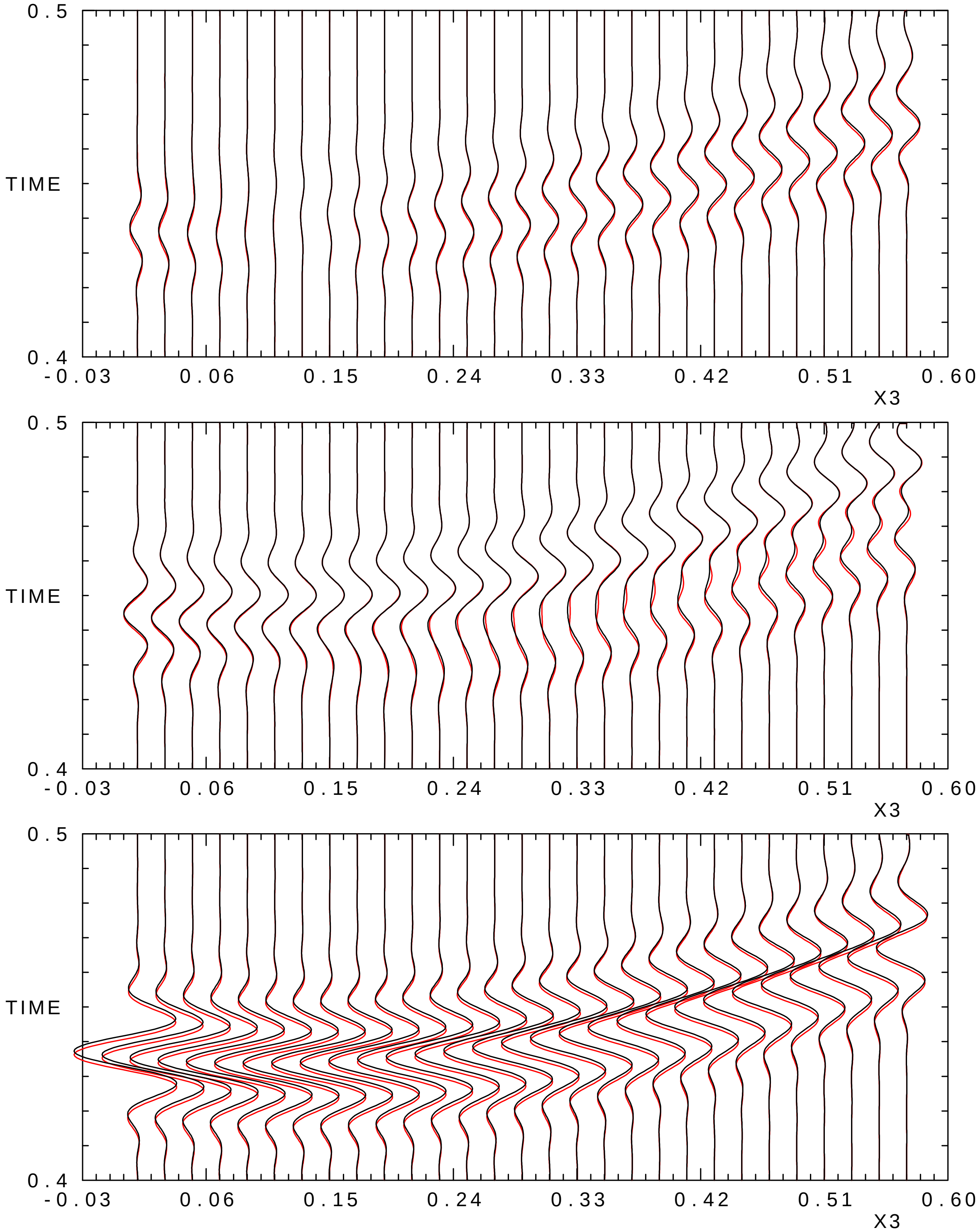

Figure 2. Coupling ray theory synthetic seismograms in model QI2. The **black** seismograms correspond to the *anisotropic reference rays*, simulated by the second–order perturbation of travel time along isotropic rays. The **red** seismograms correspond to the *isotropic common ray* approximation of the coupling ray theory. The differences due to the isotropic common ray approximation are small but already visible. From top to bottom: the first (radial) component, the second (transverse) component, the third (vertical) component.

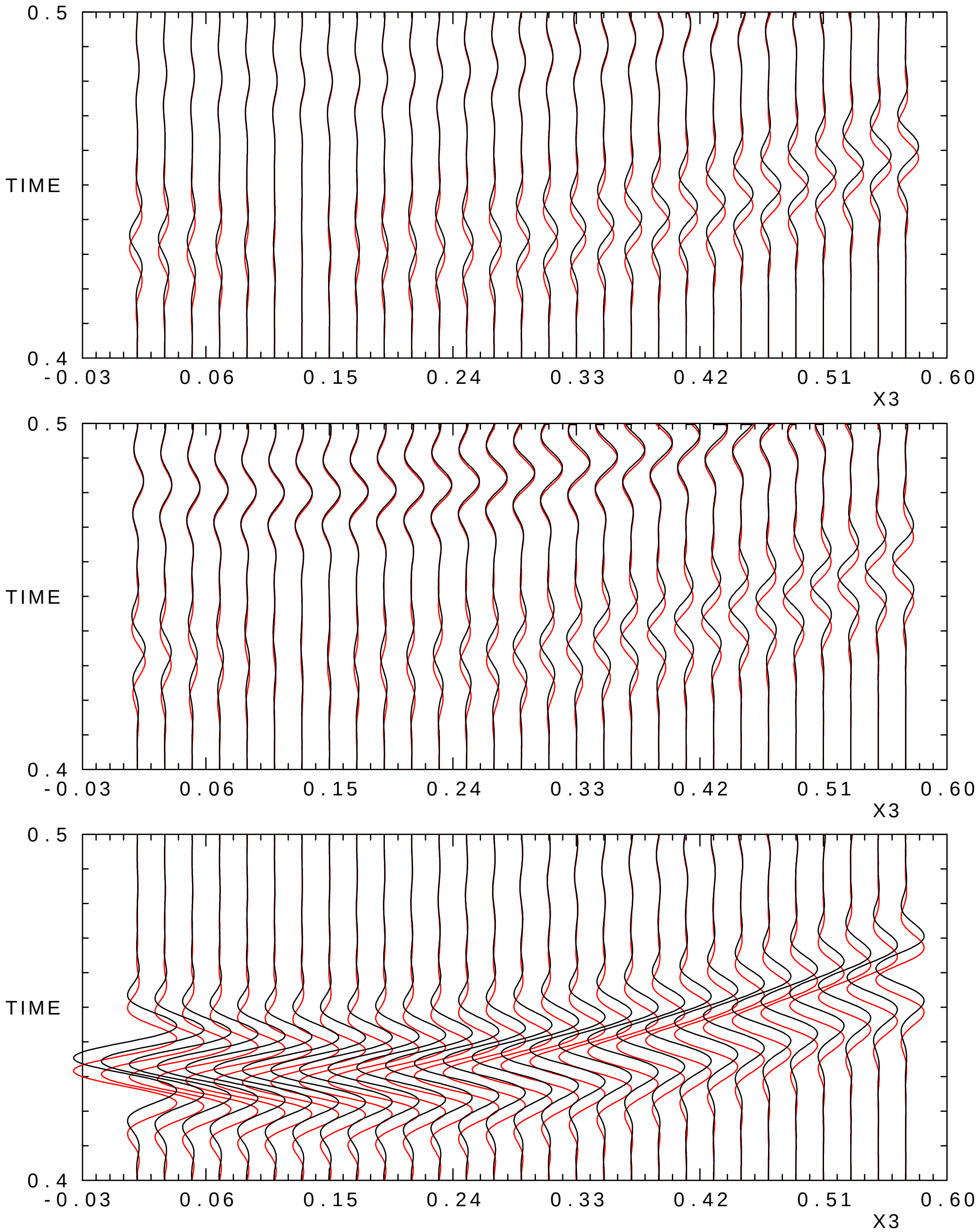

Figure 3. Coupling ray theory synthetic seismograms in model QI4. The **black** seismograms correspond to the *anisotropic reference rays*, simulated by the second–order perturbation of travel time along isotropic rays. The inaccuracy of this simulation in model QI4 roughly corresponds to the line thickness, see Table 3. The **red** seismograms correspond to the *isotropic common ray* approximation of the coupling ray theory. The differences due to the isotropic common ray approximation are considerable in this quite strongly anisotropic model QI4. From top to bottom: the first (radial) component, the second (transverse) component, the third (vertical) component.

Rec. dep.	ICR time	ICR linear terms		ICR quadratic terms		ICR remaining terms		ACR q.terms
0.01	0.440985	-0.002392	0.003983	0.000258	0.000000	0.000000	0.000006	0.000068
0.15	0.438073	-0.002518	0.004004	0.000253	0.000000	0.000013	0.000002	0.000067
0.29	0.443549	-0.002967	0.004118	0.000251	0.000000	0.000008	0.000001	0.000069
0.43	0.456330	-0.003661	0.004318	0.000248	0.000001	0.000022	0.000008	0.000072
0.57	0.475198	-0.004520	0.004595	0.000244	0.000001	0.000021	0.000008	0.000075

Table 1. First–order and second–order terms in the common ray approximations of travel time in model QI.

Rec. dep.	ICR time	ICR linear terms		ICR quadratic terms		ICR remaining terms		ACR q.terms
0.01	0.440985	-0.004747	0.011604	0.001001	0.000000	-0.000013	0.000002	0.000242
0.15	0.438073	-0.004993	0.011612	0.000979	0.000000	0.000009	0.000004	0.000236
0.29	0.443549	-0.005875	0.011837	0.000968	0.000000	0.000029	0.000001	0.000231
0.43	0.456330	-0.007234	0.012234	0.000954	0.000000	0.000063	0.000008	0.000224
0.57	0.475198	-0.008912	0.012764	0.000932	0.000000	0.000088	0.000006	0.000215

Table 2. First–order and second–order terms in the common ray approximations of travel time in model QI2.

Rec. dep.	ICR time	ICR linear terms		ICR quadratic terms		ICR remaining terms		ACR q.terms
0.01	0.440985	-0.009344	0.041578	0.003755	0.000504	0.000018	-0.000141	0.000376
0.15	0.438073	-0.009818	0.041342	0.003662	0.000562	0.000097	-0.000150	0.000339
0.29	0.443549	-0.011519	0.041461	0.003588	0.000721	0.000216	-0.000175	0.000274
0.43	0.456330	-0.014129	0.041794	0.003490	0.000952	0.000365	-0.000191	0.000200
0.57	0.475198	-0.017335	0.042241	0.003358	0.001209	0.000499	-0.000200	0.000134

Table 3. First–order and second–order terms in the common ray approximations of travel time in model QI4.

Tables 1, 2 and 3. *Rec. dep.* stands for the receiver depth along the vertical profile, see Figures 1, 2 and 3. The *ICR time* is the reference travel time τ along the isotropic common ray. The *ICR linear terms* are the linear terms $\tau_{,1}$ and $\tau_{,2}$ in Taylor expansion (17) of the anisotropic ray theory travel times in the vicinity of the isotropic common ray, and represent the travel–time corrections considered in the isotropic common ray approximation of the coupling ray theory. The *ICR quadratic terms* stand for second–order terms (18) in Taylor expansion (17) of travel time, and represent the estimates of the errors due to the isotropic common ray approximation of the anisotropic ray theory travel times. The *ICR remaining terms* stand for the difference between the exact anisotropic ray theory travel times calculated by program ANRAY version 4.40 (Gajewski & Pšenčík 1990, Pšenčík 1998b) and the second–order Taylor expansion (17), in order to illustrate the reliability of the error estimates. The *ACR quadratic terms* stand for the estimate (19) of equal quadratic terms in Taylor expansion of the anisotropic ray theory travel times in the vicinity of the anisotropic common ray, and represent the estimate of the error due the anisotropic common ray approximation (Bakker 2002) of the anisotropic ray theory travel times.

in Figure 3. The first–order anisotropic common ray approximation by Bakker (2002) seems well applicable even in this quite strongly anisotropic model QI4, and its accuracy is even better than the accuracy of the second–order Taylor expansion (17) from the isotropic common ray, see Table 3.

Although we have successfully applied the second–order perturbations of travel time to the estimation of anisotropic ray theory travel times in these simple 1-D models with constant gradients of the density–normalized elastic moduli, we cannot recommend approximation of travel time using the second–order perturbations in more complex models, because the second–order perturbations may be infinitely large in the vicinity of caustics. The second–order perturbations of travel time should be used especially for estimating and controlling the accuracy.

3.4. Comparison with the effects of other quasi–isotropic approximations

We shall now numerically compare the error due to the *isotropic common ray* (ICR) *approximation* with the errors due to the quasi–isotropic projection of the Green tensor, due to the quasi–isotropic approximation of the Christoffel matrix, and due to the quasi–isotropic perturbation of travel times.

In the *quasi–isotropic projection of the Green tensor* (Bulant & Klimeš 2002a, appendix A.2; 2002b, sec. 3.2), the S–wave coupling ray theory Green tensor is projected onto the reference polarization planes perpendicular to the reference ray. The projection is applied at the source and receiver points. The relative wavefield error due to the projection is frequency–independent and is roughly proportional to the degree of anisotropy. The coupling ray theory synthetic seismograms calculated with and without the quasi–isotropic projection of the Green tensor in models QI, QI2 and QI4 are compared in Figures 4, 5 and 6, respectively.

In the *quasi–isotropic approximation of the Christoffel matrix* (Bulant & Klimeš 2002a, appendix A.3; 2002b, sec. 3.3), the Christoffel matrix is approximated by its projections onto the reference S–wave polarization plane perpendicular to the reference ray and onto the reference P–wave polarization line tangent to the reference ray. The projection is applied along the reference ray and distorts the S–wave travel times towards the P–wave travel time. The relative wavefield error due to this approximation is proportional to frequency and is roughly proportional to the square of the degree of anisotropy. The coupling ray theory synthetic seismograms calculated with and without the quasi–isotropic approximation of the Christoffel matrix in models QI, QI2 and QI4 are compared in Figures 7, 8 and 9, respectively.

In the *quasi–isotropic perturbation of travel times* (Bulant & Klimeš 2002a, appendix A.4; 2002b, sec. 3.4), the anisotropic ray theory travel times are approximated by the linear perturbation with respect to the density–normalized elastic moduli, instead of using more accurate perturbation (2). This quasi–isotropic approximation corresponds to substituting Hamiltonian $H = -G^{-1}$, see (3), by Hamiltonian $H = \frac{1}{2}G$ (Klimeš 2002). The relative wavefield error due to this approximation is proportional to frequency and is very roughly proportional to the square of the difference between the anisotropic model and the reference isotropic model, see equation (69) below. The coupling ray theory synthetic seismograms calculated with and without the quasi–isotropic perturbation of travel times in models QI, QI2 and QI4 are compared in Figures 10, 11 and 12, respectively.

We define the relative root mean square (r.m.s.) difference between time–harmonic Green tensors $G_{ij}^{(1)}$ and $G_{ij}^{(2)}$ as

$$\rho\mathbf{G} = \sqrt{\frac{2\big(G_{ij}^{(1)} - G_{ij}^{(2)}\big)^{*}\,\big(G_{ij}^{(1)} - G_{ij}^{(2)}\big)}{\big(G_{mn}^{(1)}\big)^{*}G_{mn}^{(1)} + \big(G_{mn}^{(2)}\big)^{*}G_{mn}^{(2)}}} \quad , \tag{65}$$

where * denotes the complex conjugacy.

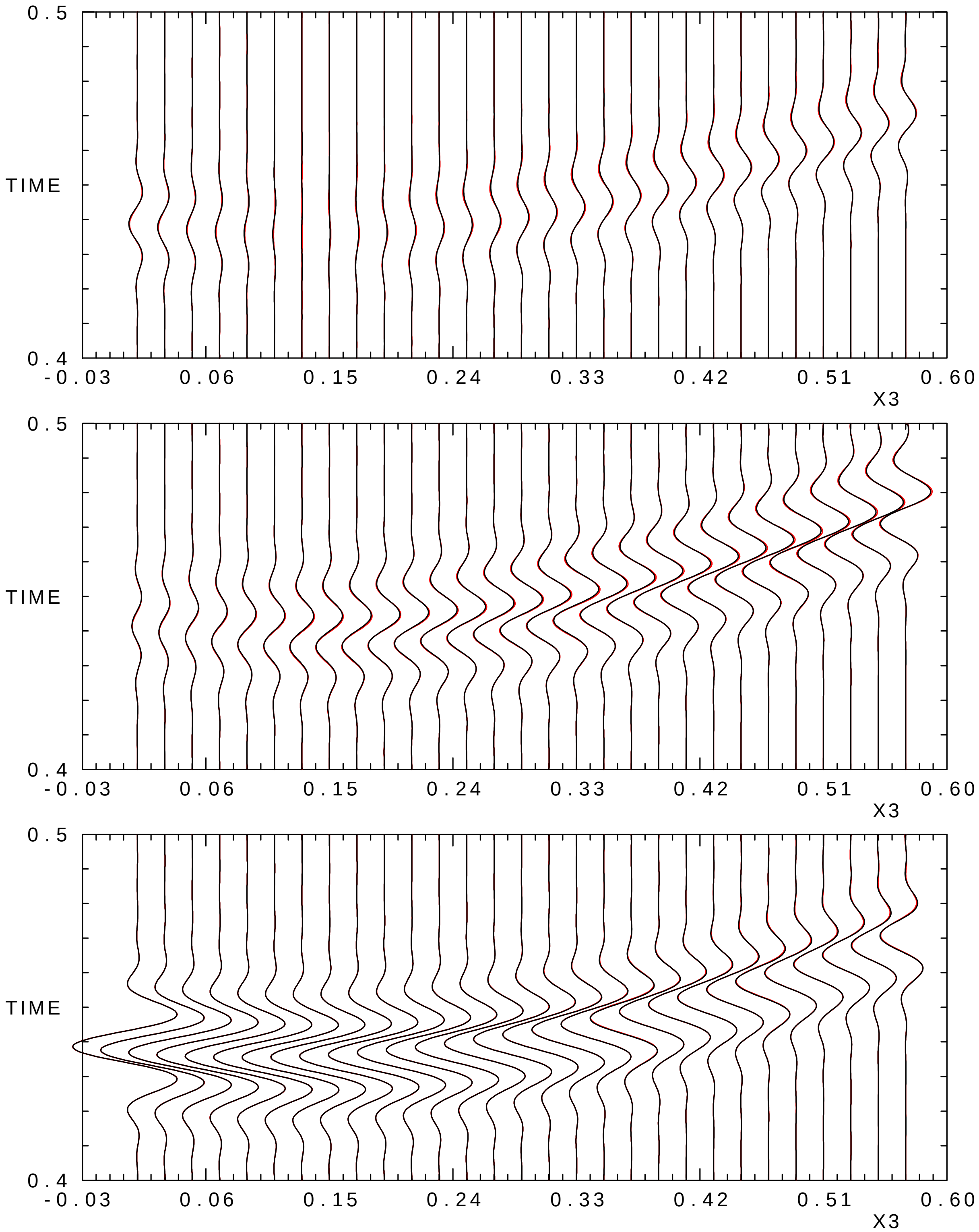

Figure 4. Quasi–isotropic projection of the Green tensor in model QI. The **red** seismograms differ from the **black** coupling ray theory synthetic seismograms by the quasi–isotropic projection of the Green tensor. The isotropic common ray approximation is applied in both cases. From top to bottom: the first (radial) component, the second (transverse) component, the third (vertical) component.

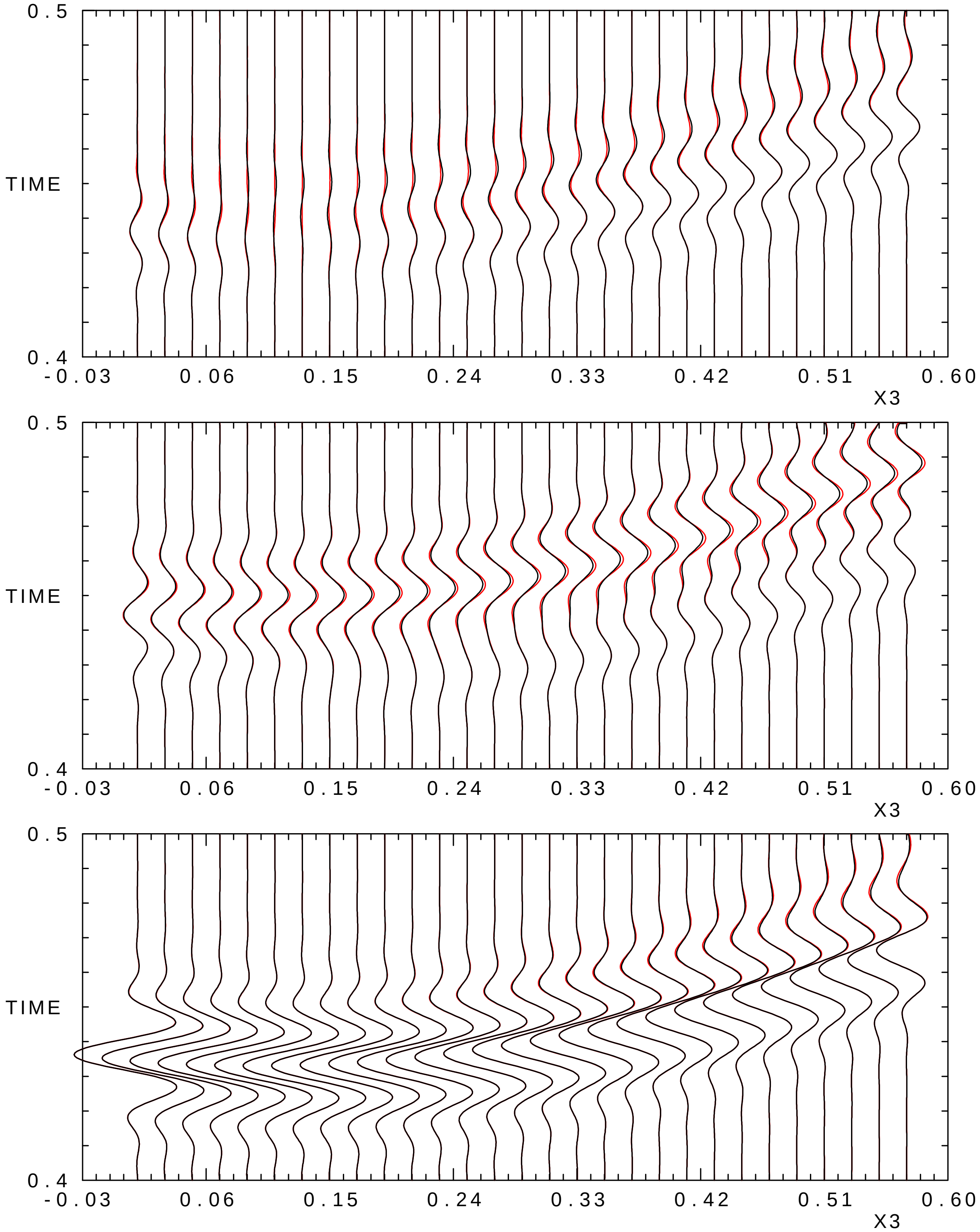

Figure 5. Quasi–isotropic projection of the Green tensor in model QI2. The **red** seismograms differ from the **black** coupling ray theory synthetic seismograms by the quasi–isotropic projection of the Green tensor. The isotropic common ray approximation is applied in both cases. From top to bottom: the first (radial) component, the second (transverse) component, the third (vertical) component.

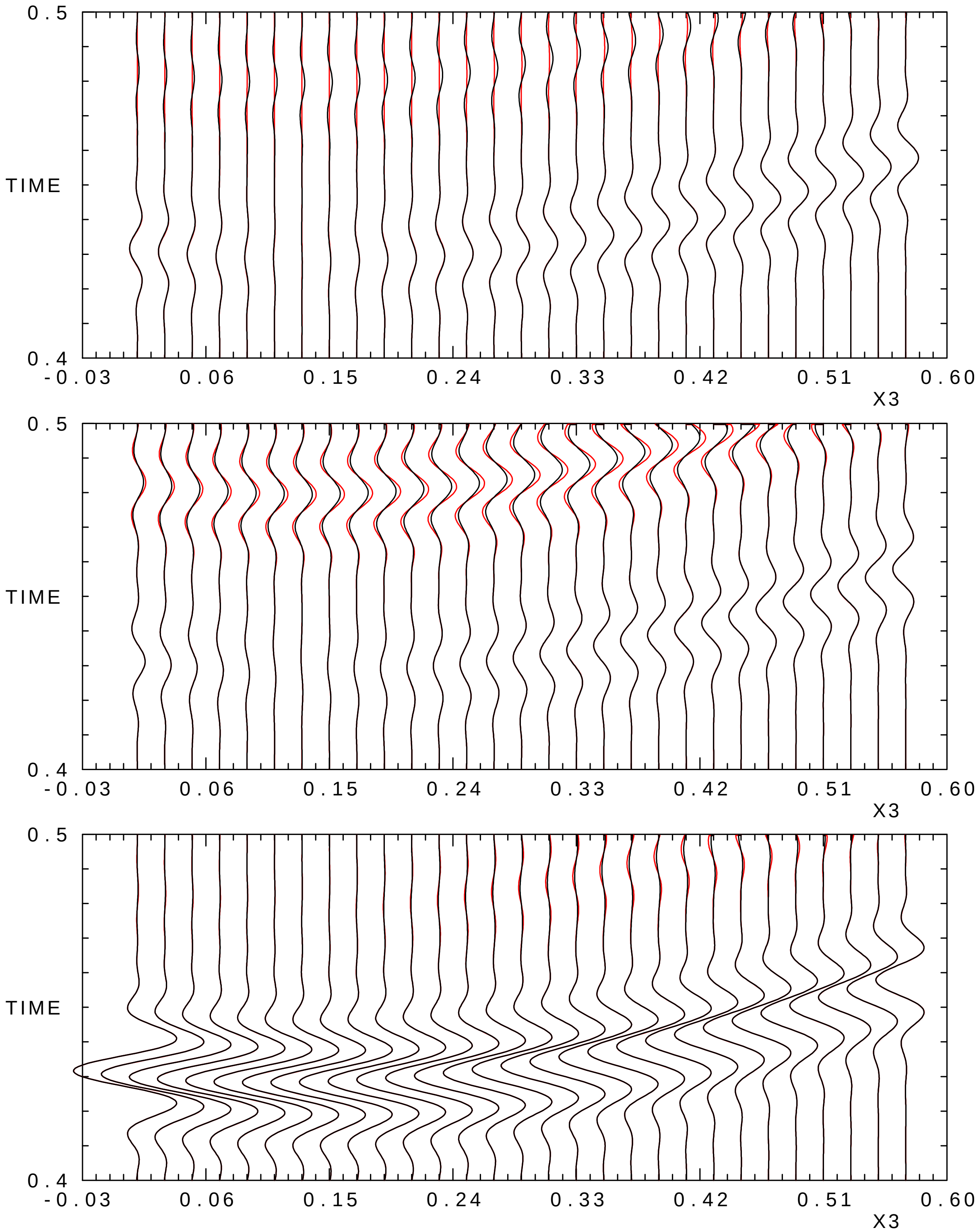

Figure 6. Quasi–isotropic projection of the Green tensor in model QI4. The **red** seismograms differ from the **black** coupling ray theory synthetic seismograms by the quasi–isotropic projection of the Green tensor. The isotropic common ray approximation is applied in both cases. From top to bottom: the first (radial) component, the second (transverse) component, the third (vertical) component.

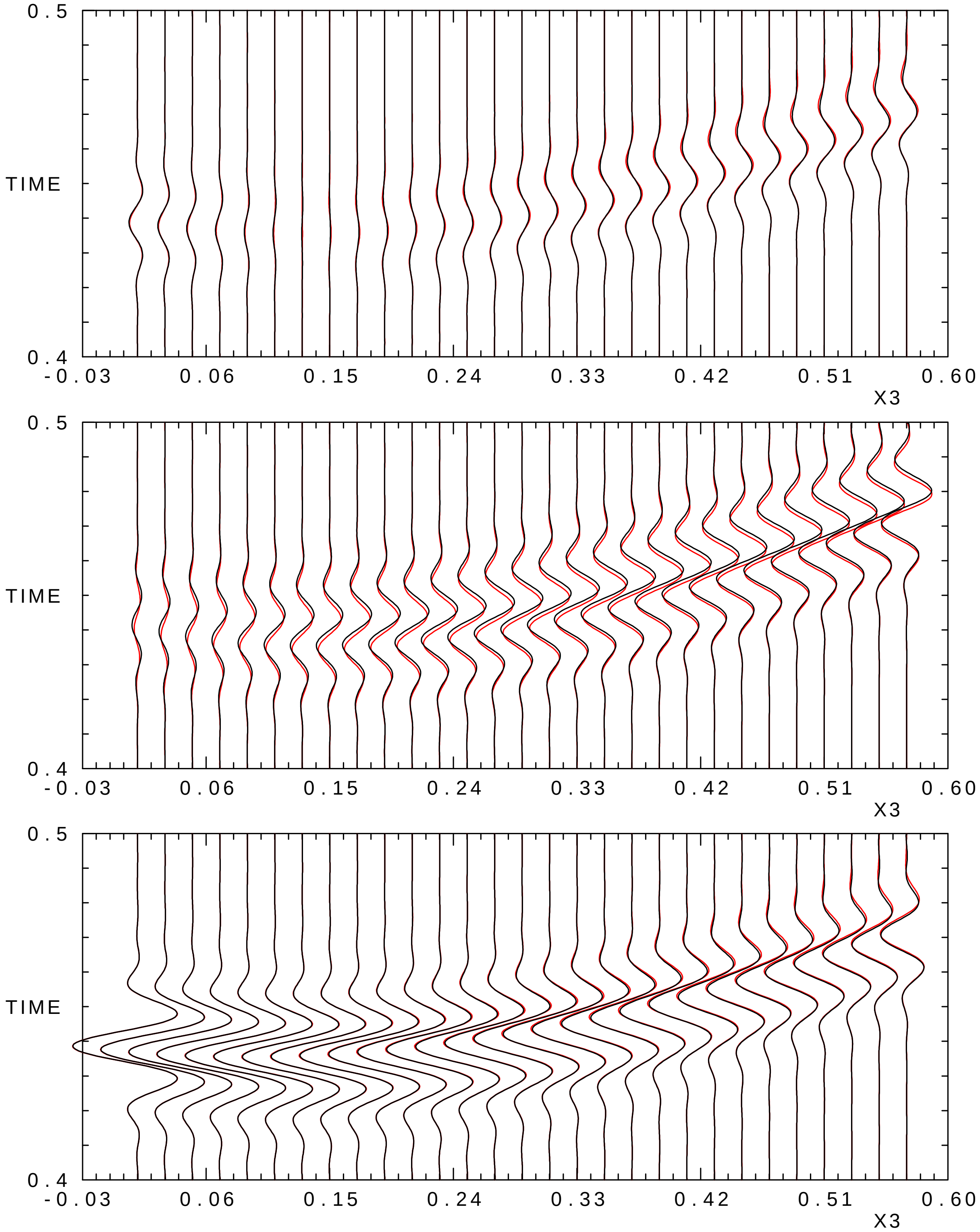

Figure 7. Quasi–isotropic approximation of the Christoffel matrix in model QI. The **red** seismograms differ from the **black** coupling ray theory synthetic seismograms by the quasi–isotropic approximation of the Christoffel matrix. The isotropic common ray approximation is applied in both cases. From top to bottom: the first (radial) component, the second (transverse) component, the third (vertical) component. Note that this impact of the quasi–isotropic approximation of the Christoffel matrix on the coupling ray theory synthetic seismograms in model QI have already been demonstrated by Bulant & Klimeš (2002a).

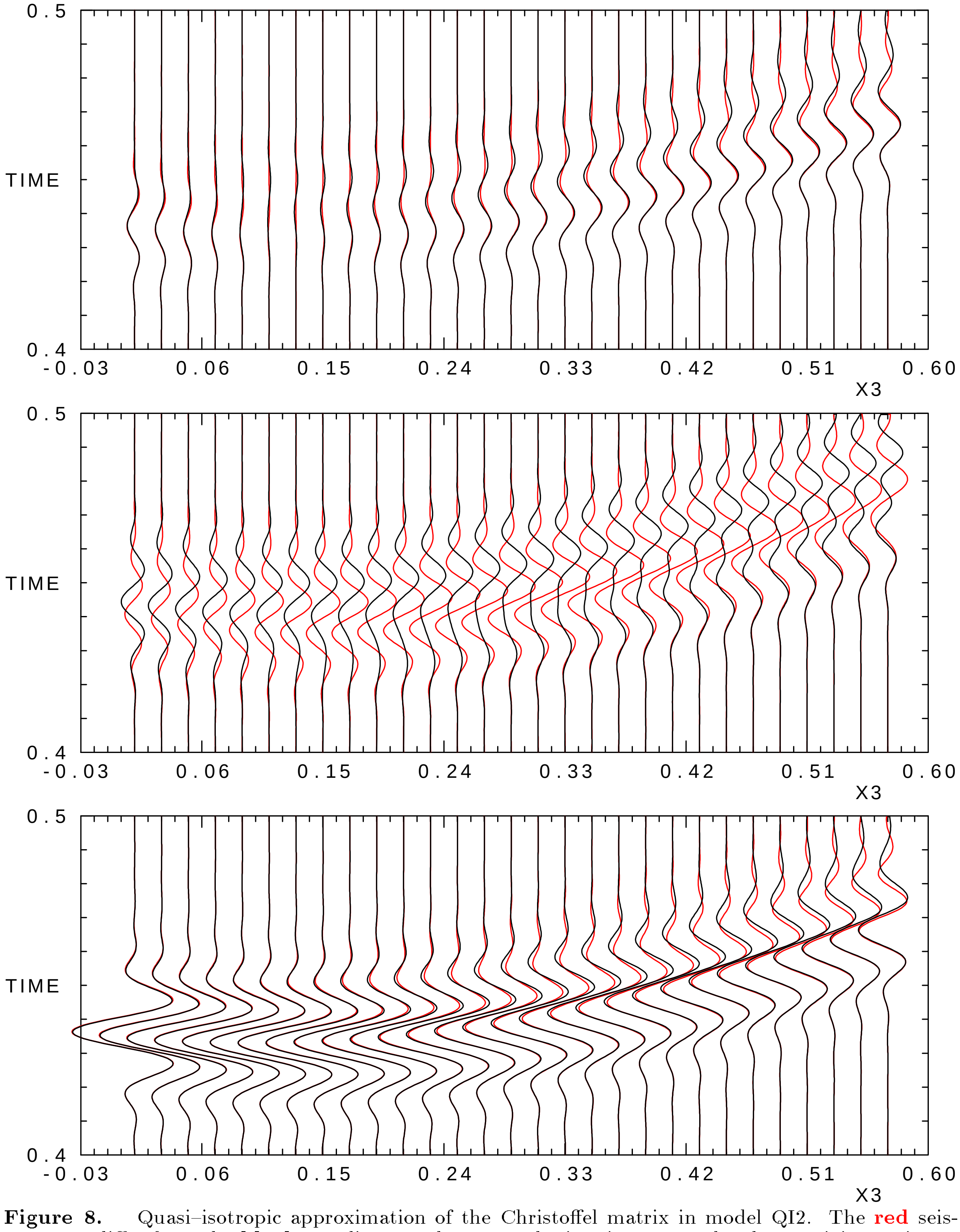

Figure 8. Quasi–isotropic approximation of the Christoffel matrix in model QI2. The **red** seismograms differ from the **black** coupling ray theory synthetic seismograms by the quasi–isotropic approximation of the Christoffel matrix. The isotropic common ray approximation is applied in both cases. From top to bottom: the first (radial) component, the second (transverse) component, the third (vertical) component.

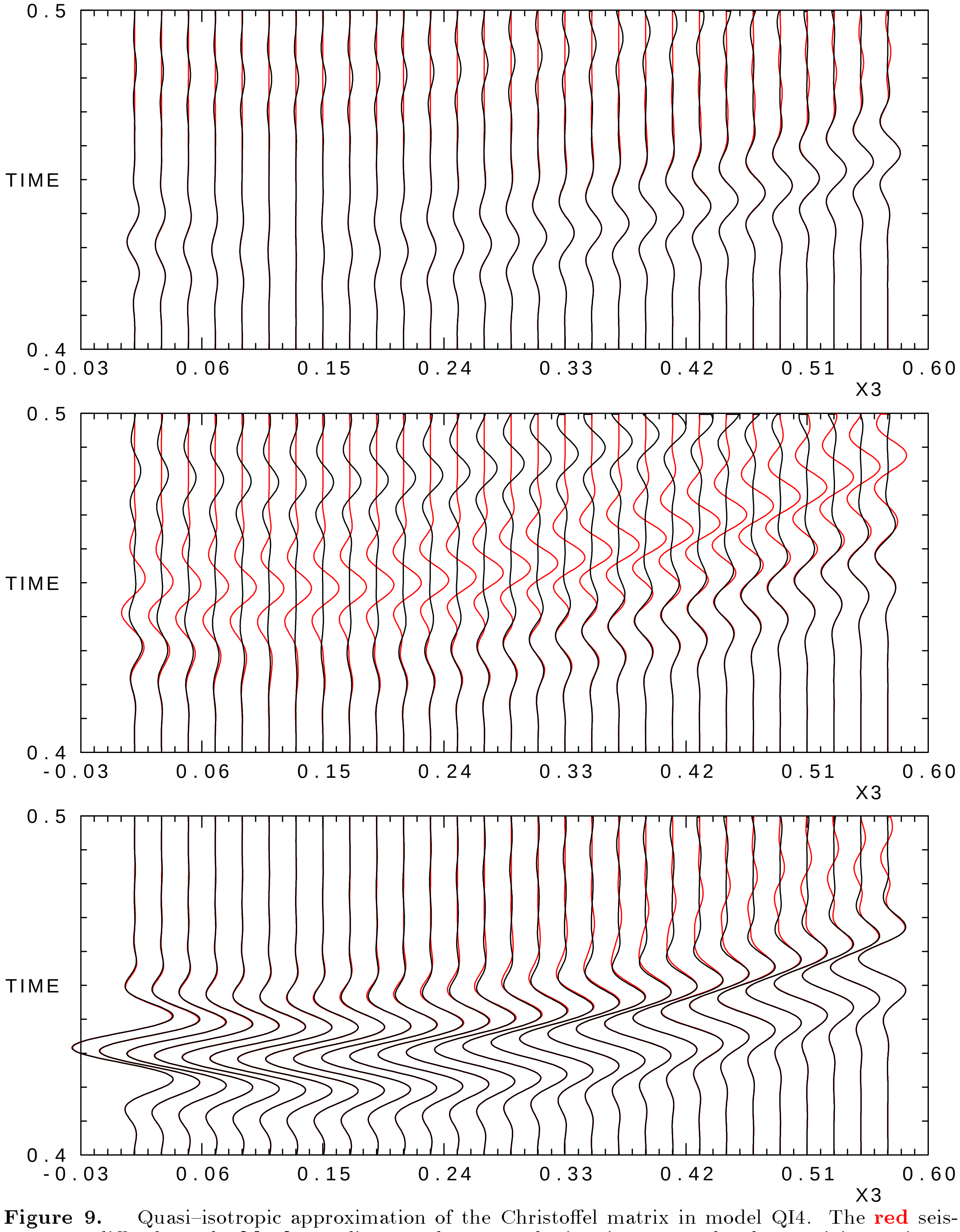

Figure 9. Quasi–isotropic approximation of the Christoffel matrix in model QI4. The **red** seismograms differ from the **black** coupling ray theory synthetic seismograms by the quasi–isotropic approximation of the Christoffel matrix. The isotropic common ray approximation is applied in both cases. From top to bottom: the first (radial) component, the second (transverse) component, the third (vertical) component.

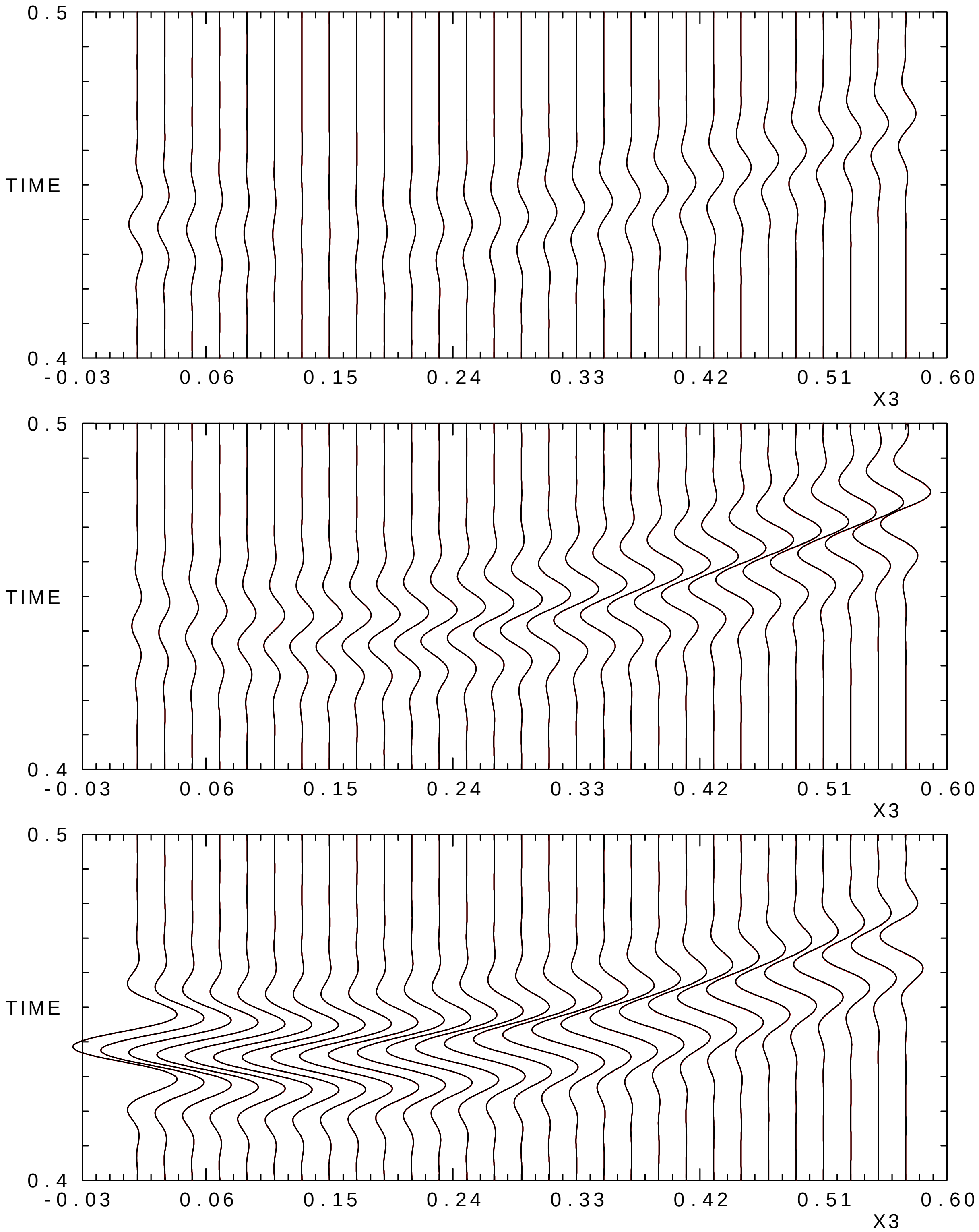

Figure 10. Quasi–isotropic perturbation of travel times in model QI. The **red** seismograms differ from the **black** coupling ray theory synthetic seismograms by the quasi–isotropic perturbation of travel times. The isotropic common ray approximation is applied in both cases. From top to bottom: the first (radial) component, the second (transverse) component, the third (vertical) component.

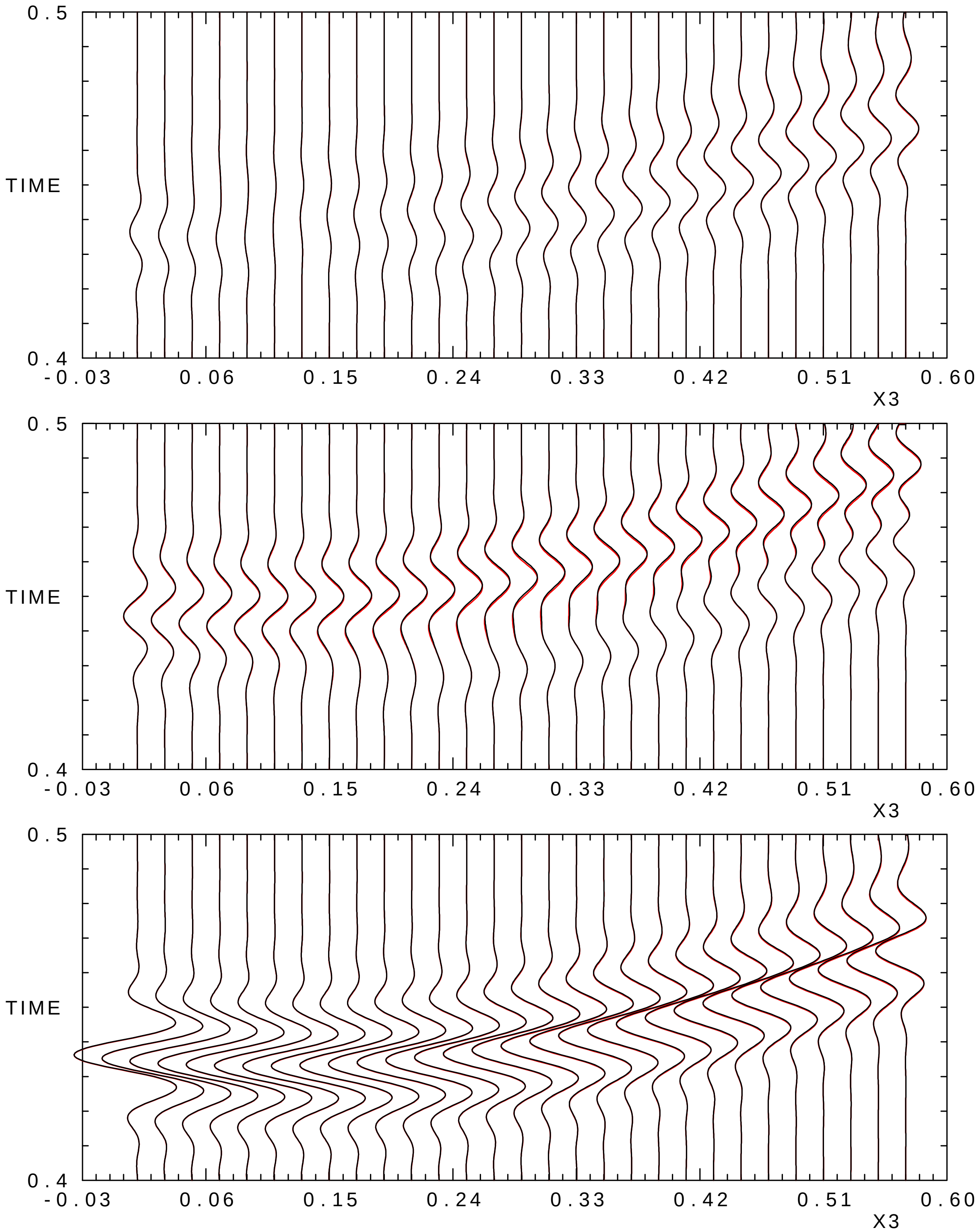

Figure 11. Quasi–isotropic perturbation of travel times in model QI2. The **red** seismograms differ from the **black** coupling ray theory synthetic seismograms by the quasi–isotropic perturbation of travel times. The isotropic common ray approximation is applied in both cases. From top to bottom: the first (radial) component, the second (transverse) component, the third (vertical) component.

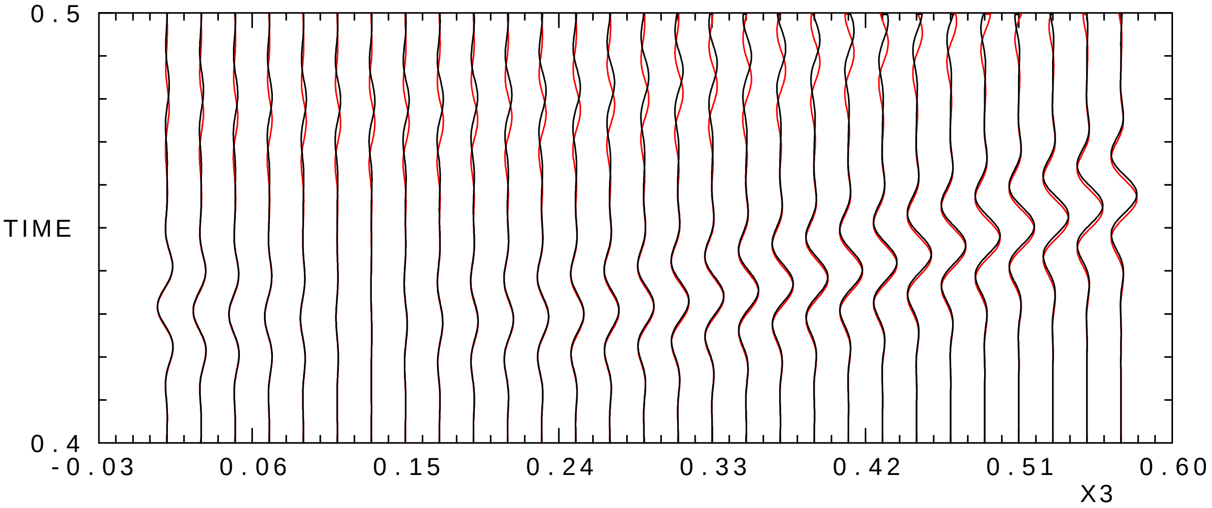

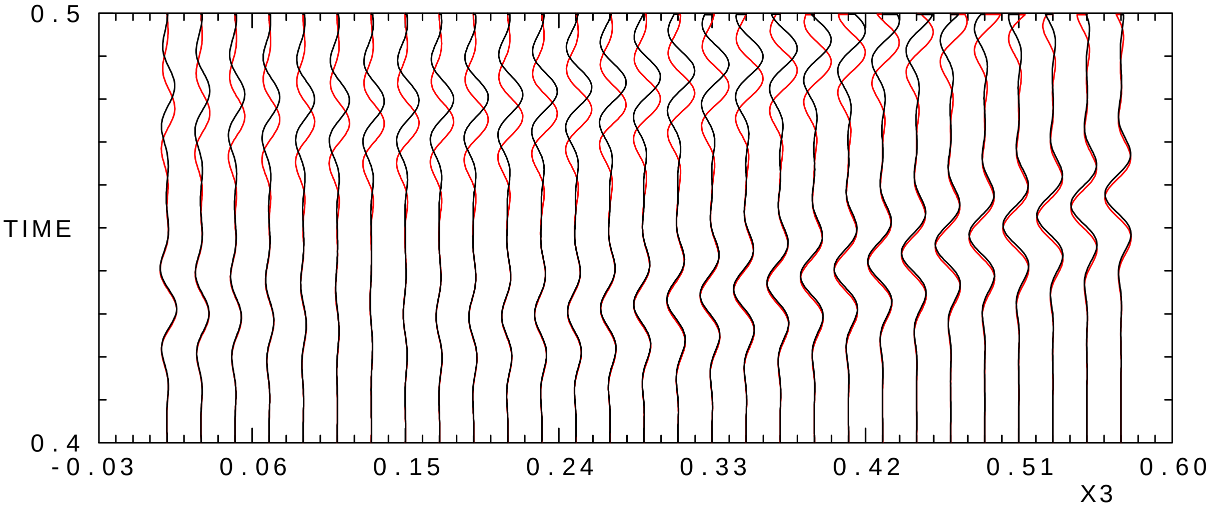

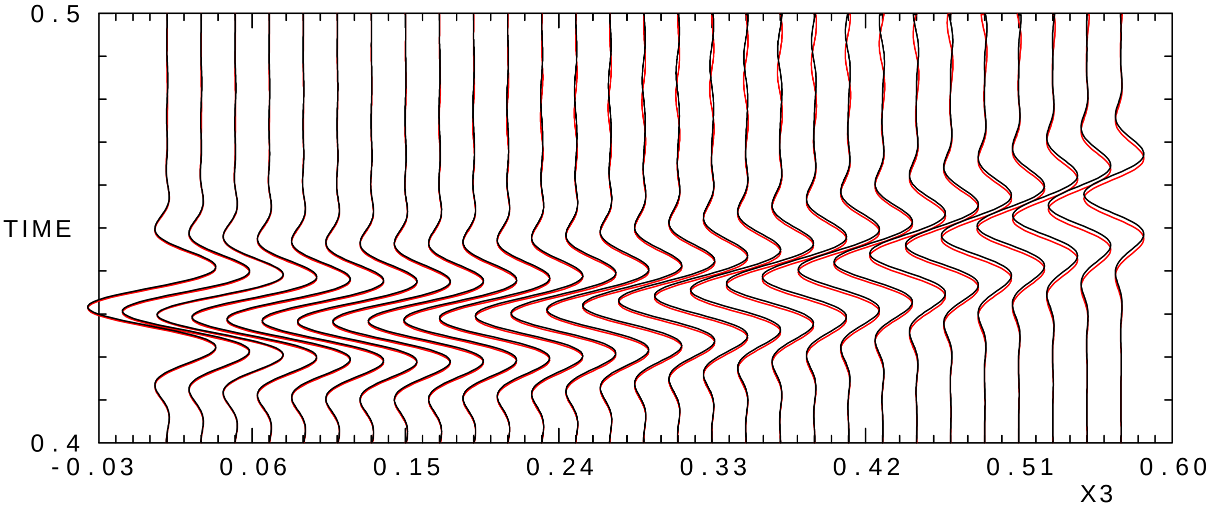

Figure 12. Quasi–isotropic perturbation of travel times in model QI4. The **red** seismograms differ from the **black** coupling ray theory synthetic seismograms by the quasi–isotropic perturbation of travel times. The isotropic common ray approximation is applied in both cases. From top to bottom: the first (radial) component, the second (transverse) component, the third (vertical) component.

Receiver depth	ICR eq. (66)	ICR eq. (68)	ICR numeric	QI project. Green t.	QI appr. Christ.m.	QI travel times	QI t.t. eq. (69)
0.01	0.057	0.057	0.057	0.061	0.348	0.013	0.012
0.15	0.056	0.056	0.056	0.061	0.347	0.013	0.012
0.29	0.056	0.056	0.055	0.061	0.350	0.014	0.014
0.43	0.055	0.055	0.055	0.060	0.355	0.017	0.017
0.57	0.054	0.054	0.054	0.058	0.358	0.021	0.021

Table 4. Relative r.m.s. error of the time–harmonic Green tensor at 50 Hz due to various quasi–isotropic approximations in model QI.

Receiver depth	ICR eq. (66)	ICR eq. (68)	ICR numeric	QI project. Green t.	QI appr. Christ.m.	QI travel times	QI t.t. eq. (69)
0.01	0.222	0.221	0.221	0.126	1.227	0.100	0.084
0.15	0.217	0.217	0.216	0.125	1.222	0.101	0.086
0.29	0.215	0.214	0.214	0.124	1.225	0.105	0.093
0.43	0.212	0.211	0.211	0.121	1.230	0.113	0.104
0.57	0.207	0.206	0.206	0.117	1.230	0.125	0.120

Table 5. Relative r.m.s. error of the time–harmonic Green tensor at 50 Hz due to various quasi–isotropic approximations in model QI2.

Receiver depth	ICR eq. (66)	ICR eq. (68)	ICR numeric	QI project. Green t.	QI appr. Christ.m.	QI travel times	QI t.t. eq. (69)
0.01	0.842	0.795	0.795	0.256	N/A	1.036	0.970
0.15	0.823	0.779	0.780	0.255	N/A	1.033	0.971
0.29	0.813	0.772	0.773	0.249	N/A	1.031	0.984
0.43	0.804	0.767	0.767	0.241	N/A	1.030	1.005
0.57	0.793	0.760	0.761	0.230	N/A	1.031	1.034

Table 6. Relative r.m.s. error of the time–harmonic Green tensor at 50 Hz due to various quasi–isotropic approximations in model QI4.

Tables 4, 5 and 6. The *receiver depth* is measured along the vertical profile, see Figures 1 to 12. *ICR eq.* (66) stands for the relative r.m.s. error of the Green tensor due to the isotropic common ray approximation, estimated from r.m.s. error of travel times using equation (66). *ICR eq.* (68) stands for the relative r.m.s. error of the Green tensor due to the isotropic common ray approximation, estimated from r.m.s. error of travel times using equation (68). *ICR numeric* is the actual relative r.m.s. error of the Green tensor due to the isotropic common ray approximation. The *QI project. Green t.* is the relative r.m.s. error of the Green tensor due to the quasi–isotropic projection of the Green tensor. The *QI appr. Christ.m.* means the relative r.m.s. error of the Green tensor due to the quasi–isotropic approximation of the Christoffel matrix. Label *QI travel times* denotes the actual relative r.m.s. error of the Green tensor due to the quasi–isotropic perturbation of travel times. *QI t.t.* (69) stands for estimate (69) of the relative r.m.s. error of the Green tensor due to the quasi–isotropic perturbation of travel times.

The relative r.m.s. error of the time–harmonic Green tensor at frequency f due to the isotropic common ray approximation can be estimated using travel–time errors (18). A rough approximation is

$$\rho\mathbf{G} = 2\,\pi\,f\,\delta\tau^{\mathrm{ICR}} \quad , \tag{66}$$

where

$$\delta\tau^{\mathrm{ICR}} = \sqrt{\frac{(\delta\tau_1^{\mathrm{ICR}})^2 + (\delta\tau_2^{\mathrm{ICR}})^2}{2}} \tag{67}$$

is the r.m.s. travel–time error of the isotropic common ray approximation. Travel–time errors $\delta\tau_\alpha^{\mathrm{ICR}}$ of the isotropic common ray approximation, given by equation (18), are labelled as the *ICR quadratic terms* in Tables 1, 2 and 3. Note that a more precise estimate is

$$\rho\mathbf{G} = \sqrt{2\{\,[\sin(\pi f \delta\tau_1^{\rm ICR})]^2 + [\sin(\pi f \delta\tau_2^{\rm ICR})]^2\,\}} \quad . \tag{68}$$

However, the difference between estimates (66) and (68) is negligible if the relative error is not extremely large. Even for the relative error (68) reaching 50%, estimate (66) gives 51%.

The relative r.m.s. error of the time–harmonic Green tensor due to the quasi–isotropic perturbation of travel times may roughly be approximated by the undervalued estimate

$$\rho\mathbf{G} = 3\,\pi f\,\frac{(\tau_{,1})^2 + (\tau_{,2})^2}{2\,\tau} \quad , \tag{69}$$

where $\tau_{,\alpha}$ are the linear perturbations in Taylor expansion (17), labelled as *ICR linear terms* in Tables 1, 2 and 3.

The relative r.m.s. errors of the time–harmonic Green tensor at frequency $f = 50\,\mathrm{Hz}$ due to the four quasi–isotropic approximations of the coupling ray theory are compared in Tables 4, 5 and 6. The error due to the isotropic common ray approximation is also compared with its estimates (66) and (68). The error due to the quasi–isotropic perturbation of travel times is compared with its estimate (69).

4. Conclusions

When using any kind of the common ray approximation of the coupling ray theory, the travel–time errors due to the applied common ray approximation should be evaluated. The travel–time errors due to the common ray approximations can be calculated using the equations proposed in this paper. If the errors of the isotropic common ray approximation exceed an acceptable limit, we can immediately decide whether the anisotropic common ray approximation (Bakker 2002) would be sufficiently accurate, or whether the anisotropic ray theory rays should be traced as reference rays for the coupling ray theory. The accuracy of the anisotropic common ray approximation by Bakker (2002) can be studied without tracing the anisotropic common rays. The numerical results suggest that the anisotropic common ray approximation by Bakker (2002) is worth coding and applying.

Acknowledgements

This research has been supported by the Grant Agency of the Czech Republic under Contract 205/01/0927, by the Grant Agency of the Charles University under Contracts 237/2001/B-GEO/MFF and 229/2002/B-GEO/MFF, by the Ministry of Education of the Czech Republic within Research Project J13/98-113200004, and by the members of the consortium "Seismic Waves in Complex 3-D Structures" (see "http://sw3d.mff.cuni.cz").

References

Arnaud, J.A. (1973): Hamiltonian theory of beam mode propagation. In: Wolf, E. (ed.): *Progress in Optics, Vol. 11*, North–Holland publ. Co.

Babich, V.M. & Buldyrev, N.J. (1972): *Asymptotic Methods in Problems of Diffraction of Short Waves* (in Russian). Nauka, Moscow.

Bakker, P.M. (2002): Coupled anisotropic shear wave raytracing in situations where associated slowness sheets are almost tangent. *Pure appl. Geophys.*, **159**, 1403–1417.

Bucha, V. & Bulant, P. (eds.) (2002): SW3D–CD–6 (CD–ROM). In: *Seismic Waves in Complex 3-D Structures, Report 12*, pp. 247–247, Dep. Geophys., Charles Univ., Prague, online at "http://sw3d.mff.cuni.cz".

Bucha, V., Bulant, P. & Klimeš, L. (eds.) (2001): SW3D–CD–5 (CD–ROM). In: *Seismic Waves in Complex 3-D Structures, Report 11*, pp. 357–357, Dep. Geophys., Charles Univ., Prague, online at "http://sw3d.mff.cuni.cz".

Bulant, P. & Klimeš, L. (2002a): Numerical algorithm of the coupling ray theory in weakly anisotropic media. *Pure appl. Geophys.*, **159**, 1419–1435, online at "http://sw3d.mff.cuni.cz".

Bulant, P. & Klimeš, L. (2002b): Comparison of quasi–isotropic approximations of the coupling ray theory with the exact solution in the 1-D anisotropic "oblique twisted crystal" model. In: *Seismic Waves in Complex 3-D Structures, Report 12*, pp. 171–184, Dep. Geophys., Charles Univ., Prague.

Červený, V. (1972): Seismic rays and ray intensities in inhomogeneous anisotropic media. *Geophys. J. R. astr. Soc.*, **29**, 1–13.

Červený, V. (2001): Seismic Ray Theory. Cambridge Univ. Press, New York.

Červený, V. & Hron, F. (1980): The ray series method and dynamic ray tracing system for three–dimensional inhomogeneous media. *Bull. seismol. Soc. Am.*, **70**, 47–77.

Červený, V., Klimeš, L. & Pšenčík, I. (1988): Complete seismic–ray tracing in three–dimensional structures. In: Doornbos, D.J. (ed.): *Seismological Algorithms*, pp. 89–168, Academic Press, New York.

Coates, R.T. & Chapman, C.H. (1990): Quasi–shear wave coupling in weakly anisotropic 3-D media. *Geophys. J. int.*, **103**, 301–320.

Gajewski, D. & Pšenčík, I. (1990): Vertical seismic profile synthetics by dynamic ray tracing in laterally varying layered anisotropic structures. *J. geophys. Res.*, **95B**, 11301–11315.

Klimeš, L. (2002): Second–order and higher–order perturbations of travel time in isotropic and anisotropic media. *Stud. geophys. geod.*, **46**, 213–248.

Luneburg, R.K. (1944): *Mathematical Theory of Optics.* Lecture notes, Brown University, Providence, Rhode Island. Reedition: University of California Press, Berkeley and Los Angeles, 1964.

Popov, M.M. & Pšenčík, I. (1978a): Ray amplitudes in inhomogeneous media with curved interfaces. *Travaux Instit. Géophys. Acad. Tchécosl. Sci. No. 454, Geofys. sborník*, **24**, 111–129, Academia, Praha.

Popov, M.M. & Pšenčík, I. (1978b): Computation of ray amplitudes in inhomogeneous media with curved interfaces. *Stud. geophys. geod.*, **22**, 248–258.

Pšenčík, I. (1998a): Green's functions for inhomogeneous weakly anisotropic media. *Geophys. J. int.*, **135**, 279–288.

Pšenčík, I. (1998b): Package ANRAY, version 4.10. In: *Seismic Waves in Complex 3-D Structures, Report 7*, pp. 403–404, Dep. Geophys., Charles Univ., Prague.

Pšenčík, I. & Dellinger, J. (2001): Quasi–shear waves in inhomogeneous weakly anisotropic media by the quasi–isotropic approach: A model study. *Geophysics*, **66**, 308–319.

Vavryčuk, V. (2001): Ray tracing in anisotropic media with singularities. *Geophys. J. int.*, **145**, 265–276.